European Journal of Immunology

TLR9 and STING agonists synergistically induce innate and adaptive type-II IFN

Burcu Temizoz[1], Etsushi Kuroda[1], Keiichi Ohata[1], Nao Jounai[2], Koji Ozasa[2], Kouji Kobiyama[2], Taiki Aoshi[2] and Ken J. Ishii[1,2]

[1] Laboratory of Vaccine Science, WPI Immunology Frontier Research Center (iFReC), Osaka University, Osaka, Japan
[2] Laboratory of Adjuvant Innovation, National Institute of Biomedical Innovation (NIBIO), Osaka, Japan

Agonists for TLR9 and Stimulator of IFN Gene (STING) act as vaccine adjuvants that induce type-1 immune responses. However, currently available CpG oligodeoxynucleotide (ODN) (K-type) induces IFNs only weakly and STING ligands rather induce type-2 immune responses, limiting their potential therapeutic applications. Here, we show a potent synergism between TLR9 and STING agonists. Together, they make an effective type-1 adjuvant and an anticancer agent. The synergistic effect between CpG ODN (K3) and STING-ligand cyclic GMP–AMP (cGAMP), culminating in NK cell IFN-γ (type-II IFN) production, is due to the concurrent effects of IL-12 and type-I IFNs, which are differentially regulated by IRF3/7, STING, and MyD88. The combination of CpG ODN with cGAMP is a potent type-1 adjuvant, capable of inducing strong T_h1-type responses, as demonstrated by enhanced antigen-specific IgG2c and IFN-γ production, as well as cytotoxic $CD8^+$ T-cell responses. In our murine tumor models, intratumoral injection of CpG ODN and cGAMP together reduced tumor size significantly compared with the singular treatments, acting as an antigen-free anticancer agent. Thus, the combination of CpG ODN and a STING ligand may offer therapeutic application as a potent type-II IFN inducer.

Keywords: Adjuvant · cGAMP · CpG ODN · IFN-γ · STING · TLR ·

Additional supporting information may be found in the online version of this article at the publisher's web-site

Introduction

Pathogen-derived factors, such as LPS or unmethylated CpG DNA (CpG), stimulate innate immune cells to produce cytokines, such as IL-12 and type-I or type-II IFNs, which help generate T_h1-type responses and cellular immunity [1, 2]. IL-12 acts on naïve $CD4^+$ T cells to drive T_h1 development and IFN-γ production [3, 4]. IFN-γ-producing T_h1 cells, in turn, are the main players in the induction of type-1 immunity, which is distinguished by high phagocytic activity [5, 6]. Moreover, T_h1 cells play key roles in the generation of antitumor immunity, helping with proper activation and effector functions of CTL, including IFN-γ production [7, 8]. Thus, agents that can induce strong T_h1-type responses, CTL, and NK cells [9] are urgently needed, as they may play critical roles in developing efficient vaccine adjuvants or immunotherapeutic agents against intracellular pathogens or cancer.

CpG oligodeoxynucleotides (ODNs) are synthetic single-stranded DNAs containing unmethylated CpG motifs with immunostimulatory properties due to their resemblance to bacterial genomes, and are recognized by TLR9 in certain types of innate immune cells [10, 11]. Upon ligand binding, TLR9 signals through the adaptor molecule MyD88, leading to production of

Correspondence: Prof. Ken J. Ishii
e-mail: kenishii@biken.osaka-u.ac.jp

IRF7-dependent type-I IFNs and NF-κB-dependent cytokines [12]. Additionally, in vivo, CpG ODNs have been reported to induce T_h1-type responses because of the types of cytokines that are induced by CpG ODNs in APCs [12]. Among the different types of CpG ODNs, D-type CpG ODNs strongly induce both type-I and type-II IFNs, but are not capable of inducing B-cell activation [12, 13]. K-type CpG ODNs (K3 CpG) strongly induce B-cell activation, resulting in IL-6 and antibody production, while they only weakly induce type-I and type-II IFNs [12, 13]. However, since D-type CpG ODNs form aggregates, only K3 CpG is available for clinical use [12, 13].

Along with microbial DNA, host DNA can also become a danger signal, specifically if it inappropriately locates in the cytosol, thereby leading to production of IFNs and proinflammatory cytokines [14, 15]. One recently identified cytosolic DNA sensor is cyclic GMP–AMP (cGAMP) synthase, which catalyzes production of a noncanonical cyclic dinucleotide cGAMP (2′3′cGAMP), containing noncanonical 2′,5′ and 3′,5′ linkages between its purine nucleosides [16]. Canonical cGAMP (3′3′) is synthesized within bacteria and differs from mammalian 2′3′cGAMP in that GMP and AMP nucleosides are joined by bis-(3′,5′) linkages [17, 18].

In addition to cGAMP, c-di-AMP and c-di-GMP, which are cyclic dinucleotides of bacterial origin, are ligands for the adaptor molecule Stimulator of IFN Gene (STING) that signals through the TBK1-IRF3 axis to induce type-I IFN production and NF-κB-mediated cytokine production [19, 20]. Recent studies have shown that these cyclic dinucleotides function as potent vaccine adjuvants due to their ability to enhance antigen-specific T-cell and humoral immune responses [21]. Nevertheless, our group previously demonstrated that a STING ligand, DMXAA, induces type-2 immune responses unexpectedly [22] via STING-IRF3-mediated production of type-I IFNs. As type-2 immune responses often fail to induce type-1 immune responses, the clinical usefulness of STING ligands, including cyclic dinucleotides, was debatable. For example, the most common adjuvant, aluminum salt (alum), lacks the ability to induce cell-mediated immunity, which is considered protective in cases of intracellular pathogen-derived diseases or cancer [23]. To overcome this limitation, alum has been combined with many different kinds of adjuvants, including monophosphoryl lipid A [24] and CpG ODN [25].

Based on the evidence described above, we tried to overcome the issues that K3 CpG and cGAMP possess individually by combining K3 CpG and 3′3′cGAMP. We investigated the immunological characteristics, potency as a vaccine adjuvant and potential as an antitumor immunotherapeutic of this combination, as well as its mechanisms of action in vitro and in vivo. In vitro, the effect of combined K3 CpG and cGAMP was analyzed using human and mouse PBMCs (mPBMCs). Additionally, the effect of this combination was analyzed in vivo via an immunization model by measuring the induction of antigen-specific T- and B-cell responses after combination immunization. Finally, we evaluated the ability of combined K3 CpG and cGAMP to suppress tumor growth in a mouse tumor model. Our results suggest that the combination of K3 CpG and cGAMP makes a potent type-1 adjuvant and a promising immunotherapeutic agent for cancer.

Results

Combination of K3 CpG and cGAMP potently induces IFN-γ in human PBMCs (hPBMCs)

K3 CpG is a humanized K-type (also known as B) CpG ODN that has been reported to induce type-1 immune responses, yet only weakly induces IFNs [13, 26]. On the other hand, while cGAMP can induce robust type-I IFNs and acts as an adjuvant [21], other STING ligands were reported to induce type-2 immune responses [22]. To overcome these known limits of K3 CpG and cGAMP, we examined the immunostimulatory properties of a combination of K3 CpG and the canonical 3′3′cGAMP in vitro in hPBMCs. After screening many cytokines using multiple hPBMCs to find interactions between TLR9- and STING-mediated signaling pathways (data not shown), we found that our combination displays potent synergism in the induction of IFN-γ, approximately 10- to 90-fold more than stimulation with K3 CpG or cGAMP alone (Fig. 1A).

Next, to identify the major IFN-γ-producing cell type in hPBMCs, we performed intracellular staining of IFN-γ in hPBMCs stimulated with K3 CpG, cGAMP, or the combination (gating strategy is shown in Supporting Information Fig. 2). Our results indicate that $CD3^-CD56^+CD16^+$ NK cells are the major producers of synergistic IFN-γ among the hPBMCs in response to the combination stimulation, while $CD8^+$ T cells and other cells produced a minimal amount of IFN-γ (Fig. 1B).

Type-I IFNs and IL-12 are capable of activating NK cells for IFN-γ production in addition to inducing type-1 immune responses [27, 28]. Therefore, we next examined the role of IL-12 and type-I IFNs in the combination-induced innate IFN-γ production in hPBMCs. Treatment with IL-12 neutralizing antibody partially reduced the synergistic IFN-γ induction by the combination stimulation (Fig. 1C). Although treatment with type-I IFN neutralizing antibody did not have any effect on the combination-induced IFN-γ production, neutralizing both type-I IFNs and IL-12 at the same time further reduced the synergistic IFN-γ production (Fig. 1C). These results suggest that IL-12 works in coordination with type-I IFNs for the synergistic production of IFN-γ by hPBMCs. Taken together, the results above indicate that, when combined, K3 CpG and cGAMP can be potent NK activators, leading to the production of large amounts of IFN-γ through mechanisms partially dependent on IL-12 and type-I IFNs.

Cellular and intracellular mechanisms of the synergistic IFN-γ induction by K3 CpG and cGAMP in mice

To examine the synergism between our TLR9 and STING agonists for early (innate) IFN-γ induction in mice, we stimulated mPBMCs in vitro with K3 CpG, cGAMP, or the combination. Large amounts of IFN-γ production were observed in a synergistic manner similar to what we observed in hPBMCs (Fig. 2A). Since IRF3 and IRF7 are the necessary downstream molecules for cGAMP- and CpG-mediated type-I IFN induction, respectively [17, 29], we examined

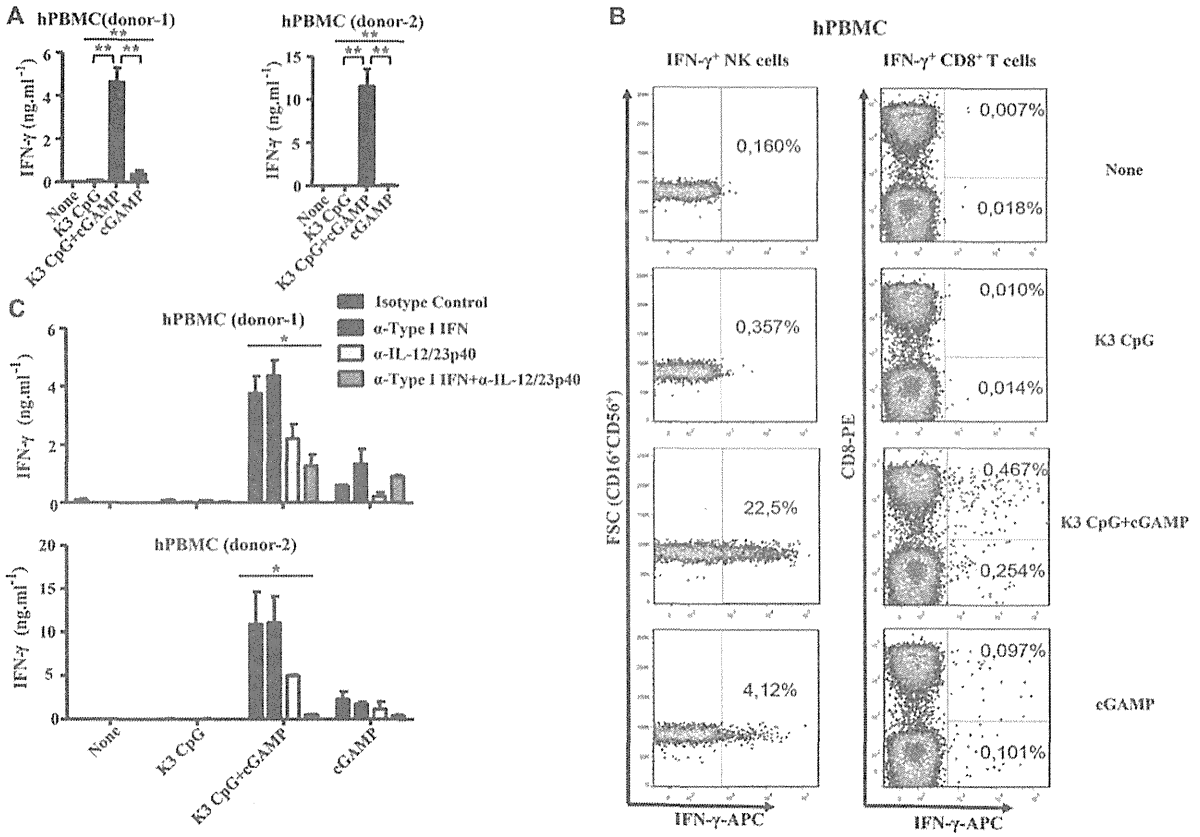

Figure 1. K3 CpG and cGAMP (TLR9 and STING agonists, respectively) synergistically induce innate IFN-γ production by human NK cells. (A) hPBMCs from two healthy donors were incubated with K3 CpG (10 μg/mL), cGAMP (10 μM), or K3 CpG (10 μg/mL) + cGAMP (10 μM) for 24 h and the supernatant IFN-γ concentrations were measured by ELISA. Data are representative of at least two independent experiments, and are shown as the mean + SD of duplicates from one experiment, representative of at least two performed. $^{*}p < 0.05$; $^{**}p < 0.01$ (one-way ANOVA with Bonferroni's multiple comparison test). (B) hPBMCs from three healthy donors were stimulated with K3 CpG, cGAMP, or K3 CpG + cGAMP for 16 h, with the last 4 h in the presence of Brefeldin A. After stimulation, cells were analyzed by flow cytometry for the detection of IFN-γ-producing cells. The percentage of IFN-γ-producing $CD3^+CD8^+$ T cells, $CD3^+CD8^-$ T cells (including $CD4^+$ T cells), and $CD3^-CD56^+CD16^+$ NK cells are indicated in the quadrants. Data from one donor, which is representative of three donors, is shown. (C) hPBMCs from two healthy donors were treated with 5 μg/mL of isotype control, type-I IFN neutralizing, IL-12/23p40 neutralizing, or type-I IFN + IL-12/23p40 neutralizing antibodies 30 min prior to 24 h of stimulation with K3 CpG, cGAMP, or K3 CpG + cGAMP. IFN-γ production was measured by ELISA. Data are representative of at least two independent experiments, and are shown as the mean + SD of duplicates from one experiment, representative of at least two performed. $^{*}p < 0.05$; $^{**}p < 0.01$ (one-way ANOVA with Bonferroni's multiple comparison test).

the roles of IRF3 and IRF7 in the synergistic IFN-γ production using mPBMCs derived from either mice deficient for both IRF3 and IRF7 (double knockout, DKO). The synergistic IFN-γ production was abrogated in the IRF3/7 DKO mPBMCs (Fig. 2A).

As IL-12 and type-I IFNs are responsible for the synergistic IFN-γ production in hPBMCs (Fig. 1C), we further examined the ability of combined K3 CpG and cGAMP to activate dendritic cells (DC) that can produce IL-12 and/or type-I IFNs. When we incubated GM-CSF-derived DCs (GM-DCs) and Flt3L-derived DCs (FL-DCs) with K3 CpG, cGAMP, or the combination, we found a similar synergy to the one we observed in mPBMCs (Fig. 2B to D). The combination of K3 CpG and cGAMP induced significantly higher IL-12p40 production by both GM-DCs (Fig. 2B) and FL-DCs (Fig. 2C), and significantly higher IFN-α production by FL-DCs (Fig. 2D) than the amounts induced by singular stimulations. This suggests a potential role for IL-12 and type-I IFNs in the synergistic IFN-γ induction by our combination. Together these results demonstrate that the synergy between K3 CpG and cGAMP that potently induces IFN-γ in hPBMCs was reproduced in mice. The mechanisms for this synergism involve IRF3/7-mediated intracellular signaling, and the synergy induces type-I IFNs by plasmacytoid DCs (pDCs) as well as IL-12 production by both conventional DCs and pDCs.

TLR9/STING agonists induce type-1 immunity, $CD8^+$ T cells, and suppress type-2 immunity

Given the presence of different kinds of agonistic STING ligands, c-di-GMP, the mammalian 2′3′cGAMP and DMXAA, which was reported to induce type-2 immune responses [18, 19, 22], we

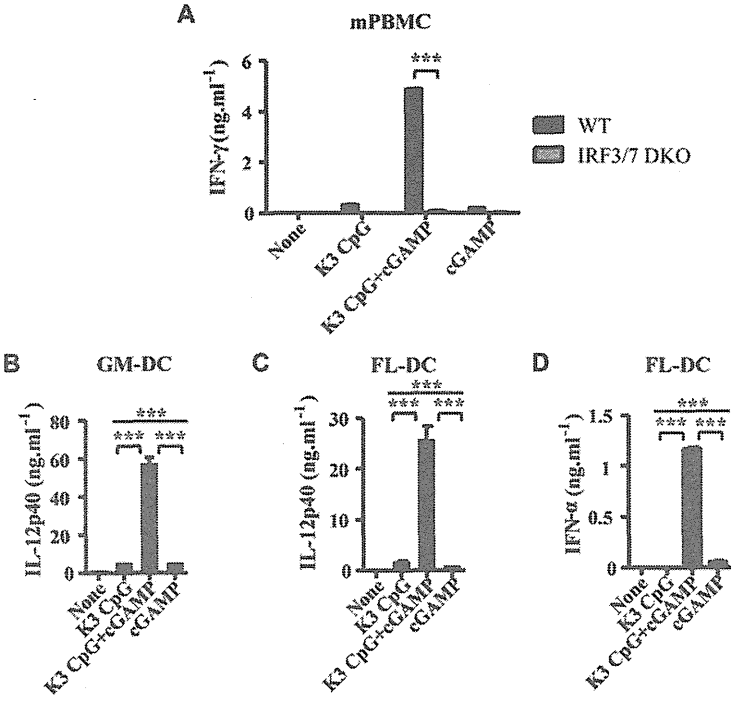

Figure 2. Combination of K3 CpG and cGAMP causes synergistic induction of innate IFN-γ in mPBMCs in an IRF3/7-dependent manner and production of IFN-α and IL-12 by DCs. (A) mPBMCs from WT and IRF3/7 DKO mice were stimulated with K3 CpG, cGAMP, or K3 CpG + cGAMP for 24 h and IFN-γ production was measured by ELISA. Data are representative of two independent experiments, and are shown as the mean + SEM of duplicates from one experiment, representative of two performed. ***$p < 0.001$ (Student's t-test); (B) GM-DCs were stimulated with K3 CpG, cGAMP, or K3 CpG + cGAMP for 24 h, and IL-12p40 production was measured by ELISA. (C and D) FL-DCs were stimulated with K3 CpG, cGAMP, or K3 CpG + cGAMP for 24 h, and (C) IL-12p40 and (D) IFN-α production were measured by ELISA. (B to D) Data are representative of two independent experiments and are shown as the mean + SD of duplicates from one experiment, representative of two performed. ***$p < 0.001$ (one-way ANOVA with Bonferroni's multiple comparison test).

next examined the ability of K3 CpG to synergize with these other STING ligands. mPBMCs stimulated with not only 3′3′cGAMP, but also 2′3′cGAMP and c-di-GMP synergized with K3 CpG to induce innate IFN-γ production (Fig. 3A).

To evaluate the adjuvant properties of these combinations in vivo, we immunized mice with the OVA protein and K3 CpG, STING agonists, or combinations of K3 CpG and STING agonists twice, at days 0 and 10. At day 17, antigen-specific antibody responses and spleen cell responses were examined. All mouse groups adjuvanted with STING agonists, such as cGAMP, c-di-GMP, and DMXAA, but not those adjuvanted with the TLR9 agonist, K3 CpG, had type-2 immune responses characterized by a high titer of serum anti-OVA IgG1 (Fig. 3B), and OVA-specific IL-13 production by splenocytes (Fig. 3C). By sharp contrast, the addition of K3 CpG converted all of the type-2 immune responses induced by STING agonists into type-1 immune responses, characterized by strong induction of OVA-specific serum IgG2c and splenocyte IFN-γ, while shutting down OVA-specific IgG1 and IL-13 production (Fig. 3B and C). We also observed synergistic induction of IFN-γ by OVA-specific $CD8^+$ T cells (Supporting Information Fig 1A). Furthermore, our in vivo CTL cytotoxicity assay (gating strategy is shown in Supporting Information Fig. 3) revealed that compared to the PBS, K3 CpG, or cGAMP immunization groups, combination of K3 CpG and cGAMP could induce strong antigen-specific $CD8^+$ CTL cytotoxicity (Supporting Information Fig. 1B) These results suggest that combinations of TLR9 and STING agonists result in potent type-1 adjuvants, capable of inducing robust $CD8^+$ T-cell responses, in addition to the induction of synergistic adaptive IFN-γ production in the antigen-stimulated spleen cells of the combination-immunized mice, and of suppressing the type-2 immune responses that are induced by STING ligands.

Synergistic induction of IFN-γ depends on IRF3/7, STING, MyD88, IL-12, and type-I IFN signaling

We showed in mPBMCs that synergistic production of innate IFN-γ was completely dependent on IRF3 and IRF7, which are required for the induction of type-I IFNs by cGAMP and K3 CpG, respectively. Since cGAMP is a ligand for STING, and K3 CpG is a ligand for TLR9 that signals via the adapter molecule MyD88, we evaluated the involvement of IRF3/7, MyD88, STING, and type-I IFNs in the combination-induced synergistic production of antigen-specific IFN-γ, using IRF3/7 DKO, IFN-α/β receptor (IFNAR) KO, MyD88 KO, and STING mutant mice. Combination-induced antigen-specific IgG2c in the sera and IFN-γ production by spleen were significantly decreased in the STING mutant, IRF3/7 DKO, MyD88 KO, and IFNAR KO mice, compared with the WT mice (Fig. 4A and B).

Our in vitro studies in mouse and hPBMCs also showed that IL-12 contributes to synergistic induction of innate IFN-γ. Therefore, we next investigated the involvement of IL-12 by using IL-12p40$^{+/-}$ and IL-12p40$^{-/-}$ mice. We found that IL-12p40 was required for the synergistic induction of antigen-specific IFN-γ, but not for the induction of IgG2c antibody responses (Fig. 4C and D). Overall our results suggest that the combination of K3 CpG and cGAMP is a potent type-1 adjuvant, synergistically inducing the production of antigen-specific IFN-γ in an IRF3/7, STING, MyD88, IL-12, and type-I IFN signaling-dependent manner.

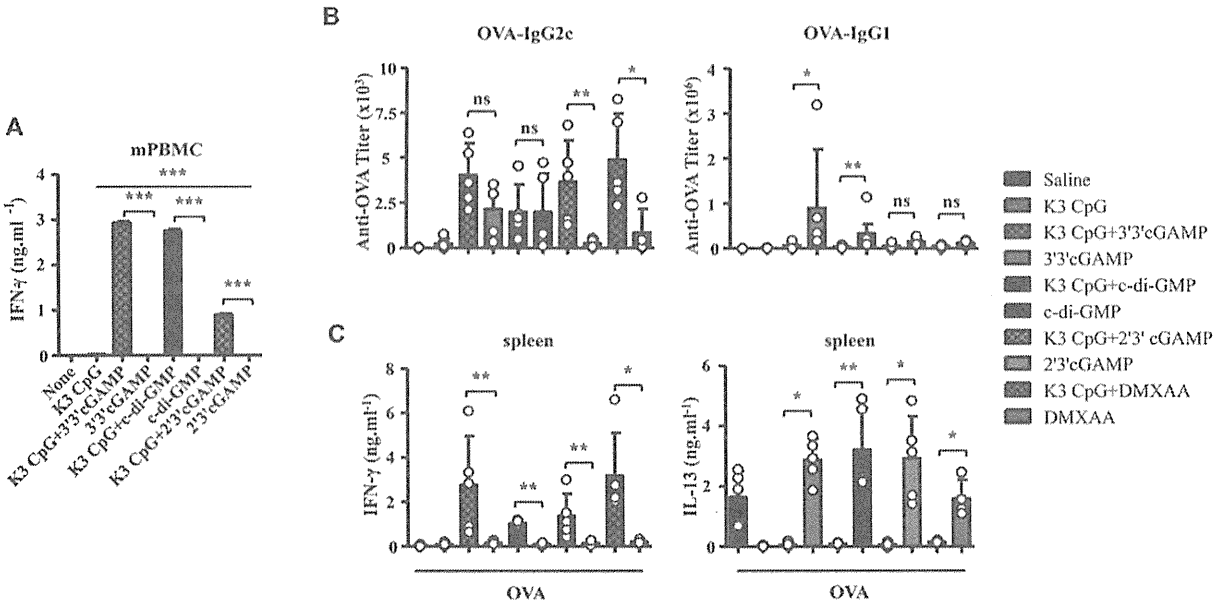

Figure 3. Combinations of TLR9 and STING agonists are potent type-1 adjuvants that also suppress type-2 immune responses in vivo. (A) mPBMCs were stimulated with K3 CpG (10 μg/mL), STING agonists (10 μM), or K3 CpG + STING agonists for 24 h and IFN-γ production was measured by ELISA. Data are representative of two independent experiments, and are shown as the mean + SEM of duplicates from one experiment, representative of two performed.*$p < 0.05$; **$p < 0.01$; ***$p < 0.001$ (one-way ANOVA with Bonferroni's multiple comparison test). (B and C) Mice ($n \geq 4$) were immunized i.m. with OVA (10 μg) with or without K3 CpG (10 μg), 3′3′/2′3′cGAMP (1 μg), c-di-GMP (1 μg), DMXAA (50 μg), or K3 + 3′3′/2′3′cGAMP/c-di-GMP/ DMXAA at days 0 and 10. (B) On day 17, OVA-specific serum IgG1 and IgG2c were measured by ELISA. (C) Spleen cells were stimulated with OVA (10 μg/mL) protein for 48 h. Production of IFN-γ and IL-13 were measured by ELISA. (B and C) Each symbol represents an individual mouse. Data are representative of two independent experiments and are shown as the mean + SD of biological replicates from one experiment, representative of two performed. *$p < 0.05$; **$p < 0.01$ (Mann–Whitney *U*-test).

Combination of K3 CpG and cGAMP efficiently suppresses tumor growth in a murine model

Because T_h1 and $CD8^+$ T-cell responses are important for the generation of antitumor immunity, we investigated the immunotherapeutic potential of the K3 CpG and cGAMP combination in a mouse tumor model. We inoculated mice with OVA-expressing EG-7 lymphoma cells by s.c. injection. On days 7 and 10, mice were given intratumor injections of PBS, K3 CpG (10 μg), cGAMP (10 μg), or K3 CpG and cGAMP. Combination treatment significantly suppressed the tumor growth compared with PBS, K3 CpG, or cGAMP treatments (Fig. 5A), suggesting that our combination can work as an antigen-free immunotherapeutic agent for cancer. In addition, the antitumor effect of the combination, in the EG-7 tumor model, was dependent on the $CD8^+$ T-cell activity, rather than the NK-cell activity, as the combination failed to suppress the tumor growth in the RAG2 KO mice (Supporting information Fig. 4B), and significantly higher amounts of IFN-γ were produced only by the OVA-specific $CD8^+$ T cells of the mice that were treated with the combination (Supporting Information Fig. 4A).

To investigate the antitumor effect of our combination in a tumor model that does not express an artificial antigen, such as OVA, we inoculated mice with B16 F10 melanoma cells that were shown to rely on NK cells for clearance [30] by s.c. injection. On days 8, 11, and 13, mice were given intratumor injections of PBS, K3 CpG (10 μg), cGAMP (10 μg), or K3 CpG and cGAMP. Although cGAMP showed a significant antitumor effect compared to the PBS treatment group, antitumor effect of the combination was the strongest among all groups (Fig. 5B).

Discussion

Efficient vaccines against intracellular pathogens or cancer require adjuvants that induce type-1 immune responses. Cyclic dinucleotides, such as cGAMP and c-di-GMP, have attracted attention as potential vaccine adjuvants because they directly bind to the transmembrane molecule STING and activate the TBK1-IRF3-dependent signaling pathway to induce type-I IFNs [31]. However, evidence that STING agonists induce type-2 immune responses [22], rather than protective type-1 immune responses, suggests that their potential therapeutic applications are limited. In this study, we solve this issue by combining STING-agonists with K3 CpG, a TLR9 ligand. This combination synergistically enhances innate and adaptive IFN-γ production. It acts as a potent type-1 adjuvant, strongly inducing antibody responses, and $CD4^+$ T_h1 and $CD8^+$ T cells, and as an antitumor agent that can efficiently suppress tumor growth in mouse tumor models of lymphoma and melanoma.

The current study demonstrates that the combination of K3 CpG and cGAMP synergistically induces innate IFN-γ production in both human and mPBMCs (Figs. 1 and 2), suggesting that this

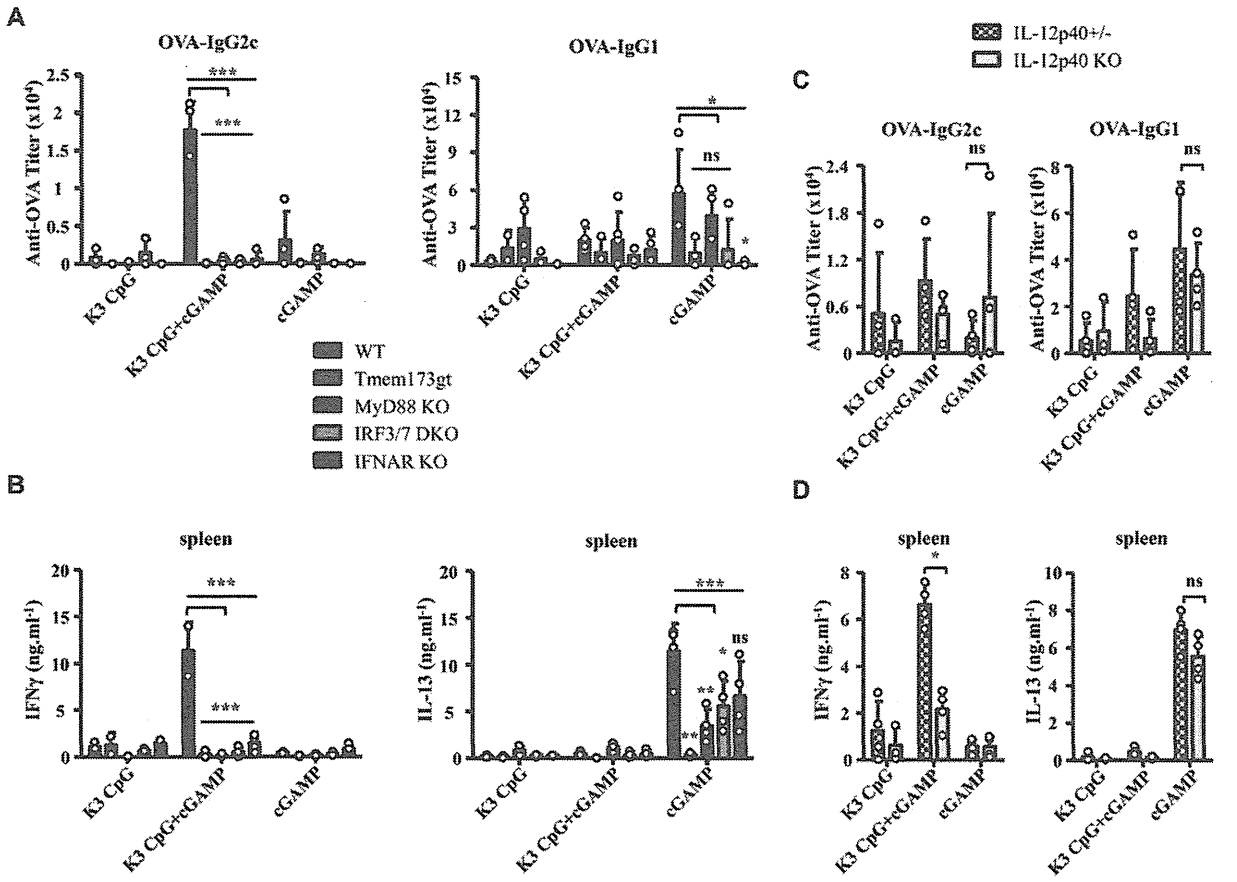

Figure 4. The synergistic effect of the combination of K3 CpG and cGAMP on antigen-specific IFN-γ induction is dependent on IRF3/7, STING, MyD88, IL-12, and type-I IFN signaling. (A) WT, Tmem173gt, IRF3/7 DKO, MyD88 KO, and IFNAR KO C57BL/6J mice ($n \geq 3$) were immunized with OVA and K3 CpG, cGAMP, or K3 + cGAMP at days 0 and 10, via the i.m. route. On day 17, OVA-specific serum IgG2c and IgG1 were measured by ELISA. Each symbols represent an individual mouse and data are representative of two independent experiments and are shown as the mean + SD of biological replicates from one experiment, representative of two performed. $^{*}p < 0.05$; $^{**}p < 0.01$; $^{***}p < 0.001$ (one-way ANOVA with Bonferroni's multiple comparison test). (B) Spleen cells from immunized mice were stimulated with OVA for 48 h. Production of IFN-γ and IL-13 were measured by ELISA. Data are representative of two independent experiments and are shown as the mean + SD of biological replicates from one experiment, representative of two performed. $^{*}p < 0.05$; $^{**}p < 0.01$; $^{***}p < 0.001$ (one-way ANOVA with Bonferroni's multiple comparison test). (C) IL-12p40 +/– and –/– C57BL/6J mice were immunized with OVA and K3 CpG, cGAMP, or K3 CpG + cGAMP at days 0 and 10, via the i.m. route. On day 17, OVA-specific serum IgG2c and IgG1 were measured by ELISA. Data are representative of two independent experiments and are shown as the mean + SD of biological replicates from one experiment, representative of two performed. $^{*}p < 0.05$ (Mann–Whitney *U*-test). (D) Spleen cells were stimulated with OVA protein for 48 h. Production of IFN-γ was measured by ELISA. Data are representative of two independent experiments and are shown as the mean + SD of biological replicates from one experiment, representative of two performed. $^{*}p < 0.05$ (Mann–Whitney *U*-test).

phenomenon is conserved between human and mouse. Importantly, combination stimulation does not affect cell viability (Supporting Information Fig. 5), which may affect cytokine production. Our in vitro results also demonstrate that the mechanisms of action involve IL-12 and type-I IFNs. Specifically, during the synergism between K3 CpG and cGAMP, type-I IFNs were dispensable since the loss of their effect can be compensated by the increased production of IL-12 (Fig. 1C and Supporting Information Fig. 6B). A previous report suggested that type-I IFNs and IL-12 can synergistically induce IFN-γ production by $CD4^+$ T cells after Listeria monocytogenes infection. They showed that the synergy was significantly decreased in the absence of both cytokines, but partially decreased in the absence of either one of the cytokines, which is consistent with our results [32]. Moreover, we found that, similar to the synergy observed in PBMCs, our combination can synergistically induce IL-12p40 production in GM-DCs and FL-DCs (Fig. 2C and D), suggesting a potential role for conventional and plasmacytoid DCs in the combination-induced synergy. A similar IL-12 synergy was reported by Krummen et al. by the combination of TLR ligands, CpG and Poly I:C, in BM-derived DCs that required the combination of MyD88- and TRIF-dependent signaling pathways [33]. Our results also demonstrate that the combination of molecules activating MyD88-dependent (TLR9) and independent (STING) signaling pathways results in a robust immunostimulatory agent, suggesting that such combinations might be useful for immunotherapeutic applications.

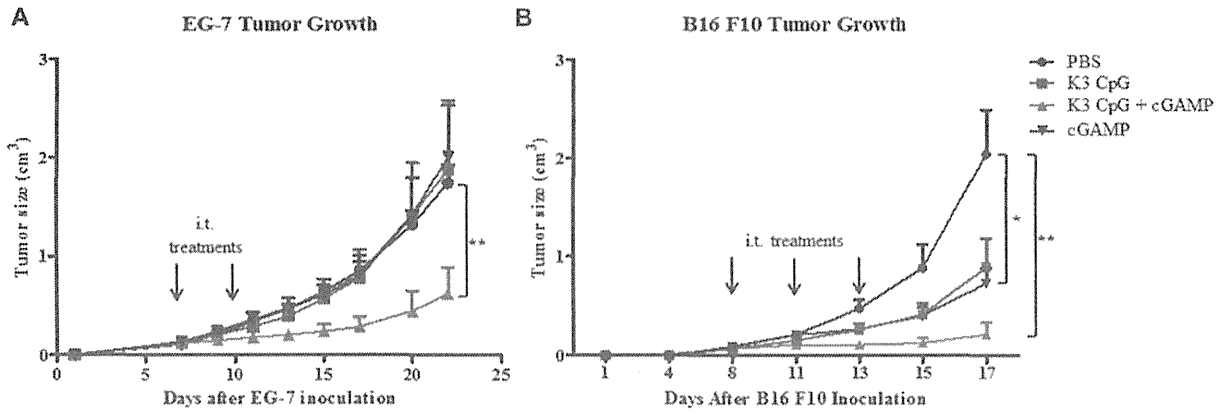

Figure 5. The combination of K3 CpG and cGAMP efficiently suppresses tumors in the EG-7 and B16 F10 mouse tumor models. (A) Mice were injected with 1×10^6 EG-7 lymphoma cells (in 100 μL of PBS) s.c. on day 0. On days 7 and 10, mice were given intratumor injections of PBS ($n = 8$), K3 CpG ($n = 8$), cGAMP (n = 8), or K3 CpG + cGAMP ($n = 9$), and were monitored for tumor growth for 22 days. (B) Mice were injected with 0.5×10^6 B16 F10 cells (in 100 μL of PBS) s.c. on day 0. On days 8, 11, and 13, mice were given intratumor injections of PBS ($n = 8$), K3 CpG ($n = 8$), cGAMP ($n = 8$), or K3 CpG + cGAMP ($n = 8$), and mice were monitored for tumor growth for 17 days. Data are representative of two independent experiments and are shown as the mean + SEM of biological replicates from one experiment, representative of two performed. $^*p < 0.05$; $^{**}p < 0.01$ (Mann–Whitney *U*-test).

According to our findings, NK cells are the major IFN-γ-producing cells in the hPBMC culture following combination stimulation (Fig. 1B). On the other hand, previous reports have shown that although NK cells express low levels of TLR9, cells that respond to CpG stimulation are the TLR9-expressing pDCs and B cells in hPBMCs [34]. Also, IL-12 and type-I IFNs have been reported to regulate IFN-γ production and cytotoxicity in NK cells [28, 35]. Given those reports and our in vitro data, our proposed mechanism for the synergistic induction of innate IFN-γ is that mainly pDCs may respond to K3 CpG, while, together with pDCs, other cells, such as conventional DCs or macrophages, may respond to cGAMP to produce high amounts of type-I IFNs and IL-12, which then synergize to induce IFN-γ production in NK cells, by signaling through IL-12 and type-I IFN receptors (Supporting Information Fig. 6A).

The first report about the adjuvant effect of 2′3′cGAMP showed that i.m. cGAMP immunization can induce antigen-specific B- and T-cell responses in a STING-dependent manner [21]. Our in vivo immunization studies using 3′3′cGAMP are also consistent with the previous reports; it induces strong antigen-specific B- and T-cell responses in a STING-dependent manner (Fig. 4A and B). We also showed that 3′3′cGAMP is a type-2 adjuvant that can induce not only IgG1, but also IgG2c antibody responses and T_h2-type cytokine responses in spleen cells (Fig. 3B and C). Although type-2 adjuvants do not usually induce the production of T_h1-like Ig isotype (IgG2c), cGAMP can do so, probably due to its ability to induce type-I IFNs, since type-I IFNs induce IgG2c antibody responses [36]. Moreover, we found that distinct mechanisms were involved in the induction of B- and T-cell responses by cGAMP, in which cGAMP-induced antibody responses, but not T_h2 responses, were dependent on type-I IFN signaling (Fig. 4B). In addition, because cGAMP is known to signal only through the STING-IRF3 axis to induce type-I IFN production [17], we expected to observe the loss of antibody and T-cell responses in IRF3/7 DKO mice. However, while cGAMP-induced antibody responses were slightly reduced in the IRF3/7 DKO mice, cGAMP-induced T-cell responses were partially dependent on IRF3/7 and, surprisingly, on MyD88, although such effects were completely dependent on STING (Fig. 4A and B). Therefore, we are further investigating the possibility that in addition to the STING-IRF3 pathway, cGAMP might activate an unknown signaling pathway that involves the adapter molecule MyD88.

Although K3 CpG was reported as an adjuvant capable of inducing type-1 immune responses [37], we found that K3 CpG by itself was a weak type-1 adjuvant, as it failed to induce antigen-specific antibody or T-cell responses at levels comparable with the cGAMP or combination immunization groups (Fig. 3B and C). Interestingly, the combination of a weak type-1 adjuvant, K3 CpG, with a type-2 adjuvant, cGAMP, resulted in a strong type-1 adjuvant that induced synergistic antigen-specific IFN-γ production and strong T_h1-like antibody and $CD8^+$ T-cell responses (Fig. 3 and Supporting Information Fig. 1). Our findings are also consistent with a previous study showing that the combination of CpG and IFA, a type-2 adjuvant, induces type-1 immune responses while suppressing type-2 immune responses [37]. Importantly, in addition to the induction of potent type-1 immune responses by our combination, we showed that it can also suppress the type-2 responses that are induced by cGAMP that is important for increased safety as dominant type-2 responses have been reported to cause a number of chronic diseases, such as allergy [5, 38, 39]. Our results are also consistent with the findings of Lin et al., in that production of IgG2c was enhanced while the production of IgG1 was suppressed by CpG [40]. Furthermore, the synergistic effect of our combination on antigen-specific IFN-γ induction is dependent on IRF3 and IRF7 (Fig. 4A and B), indicating that type-I IFNs may also play an important role in this synergy. This idea is further supported by the complete abolishment of synergy that we observed in IFNAR KO mice (Fig. 4A and B). Moreover, because MyD88 is a

downstream signaling molecule of TLR9 and cGAMP is a ligand of STING, we found that the type-1 immunity-inducing effect of the combination is dependent on both MyD88 and STING, as expected (Fig. 4A and B). On the other hand, we showed that IL-12p40 is required for the synergistic induction of T_h1-type cytokine responses, but not for the induction of IgG2c antibody responses (Fig. 4C and D). Because IL-12 is important for T_h1-cell development and IFN-γ production [3, 4], it is reasonable to observe IL-12 dependency in the T_h1-type cytokine responses. A possible explanation for the IL-12-independent IgG2c induction by our combination could be that production of type-I IFNs in the KO mice might be compensating for the absence of IL-12. Previous reports showed that type-I IFNs can induce IgG2c antibody responses in a T-cell-independent manner [36], while IL-12 induces IgG2c antibody responses by inducing IFN-γ production from T or NK cells [41]. In addition, use of anti-IL-12/23p40 neutralizing antibodies in our in vitro studies and IL-12p40 mice in the in vivo studies cannot rule out the possible involvement of IL-23 in the mechanisms of innate or adaptive IFN-γ synergy, as IL-23 signaling, which was shown to affect NK-cell activation and T-cell responses [42, 43], will be defective in both experimental designs. Our studies regarding this issue showed that although no antigen-specific IL-17 was detected in the spleen cell cultures of the immunized mice as an indirect indicator of in vivo IL-23 induction, and no IL-23 was induced in mPBMCs by combination stimulation, IL-23 is induced in the FL-DCs only by combination stimulation, but not by cGAMP or K3 CpG stimulations (data not shown), suggesting a possible role for IL-23 in the mechanisms of innate or adaptive IFN-γ synergy, which needs further investigation.

Finally, we found the K3 CpG and cGAMP combination has a strong antitumor effect, as only treatment with the combination could efficiently suppressed tumor growth in the EG-7 mouse tumor model (Fig. 5A). Because our in vivo results show that the combination induces strong $CD8^+$ T-cell responses (Supporting Information Fig. 1A and B), and the antitumor effect of the combination is lost in the RAG2 KO mice (Supporting Information Fig. 4B), which lacks $CD8^+$ T cells, we concluded that the antitumor effect of our combination is due to the induction of robust $CD8^+$ cytotoxic T-cell activation. Our hypothesis is supported by a previous report showing that vaccination with OVA-conjugated CpG ODN also has potent antitumor effects, which are dependent on $CD8^+$ T cells [44]. Moreover, since we identified NK cells as the main players in the IFN-γ synergy in our in vitro hPBMC studies, we also investigated the antitumor effect of our combination in the B16 F10 mouse melanoma tumor model, which relies on NK cells for clearance [30] and does not express artificial antigens. Although cGAMP, itself, could significantly suppress the tumor growth compared to the control group, combination had the strongest antitumor effect, resulting in almost complete tumor elimination (Fig. 5B). Thus, our combination is a strong antitumor agent, capable of suppressing tumors that relies not only on $CD8^+$ T cells, but also on NK cells for clearance. Furthermore, the advantage of our combination therapy over previously reported CpG-based antitumor agents, such as OVA-conjugated CpG ODN [44] or nanoparticle-conjugated CpG ODN [45], is that it does not require a chemical conjugation between K3 CpG and cGAMP. Additionally, unlike those systems, our approach does not require the injection or conjugation of a tumor antigen. It works as an antigen-free antitumor agent rather than a preventive vaccine.

In conclusion, our study suggests that combination of TLR9 and STING agonists is an advantageous type-1 adjuvant for vaccines requiring strong cellular immune responses, and a promising antitumor agent that can also stimulate human NK cells for synergistic IFN-γ production. Thus, our results provide insight into the mechanisms of the combined action of TLR9 and STING signaling pathways, which potentially promote the immunotherapeutic and adjuvant properties of our combination.

Materials and methods

Mice

Seven- to ten-week-old female C57BL/6J mice were purchased from CLEA Japan, Inc. (Osaka, Japan). MyD88 KO mice were purchased from Oriental BioService, Inc. (Kyoto, Japan). IL-12p40 KO and STING mutant mice (Tmem173gt), which have a loss-of-function mutation at the ligand-binding site of STING [46], were purchased from Jackson Laboratories (Bar Harbor, ME, USA). IRF3/7 DKO mice were generated from IRF3 KO [22] and IRF7 KO mice, the latter of which was provided by the RIKEN BRC (Ibaraki, Japan) via the National Bio-Resource Project of the MEXT, Japan [47]. IFNAR2 KO mice were obtained from B&K Universal. All of the animal experiments were conducted according to the guidelines of the Animal Care and Use Committee of RIMD and IFReC of Osaka University, and the use of animals was approved by Osaka University.

Reagents

The 2′3′ and 3′3′ cGAMPs were purchased from Invivogen (San Diego, CA, USA). DMXAA was purchased from Sigma-Aldrich (St. Louis, MO, USA) and dissolved in 5% $NaHCO_3$. Yamasa (Chiba, Japan) kindly donated c-di-GMP. OVA was purchased from Kanto Chemical (Osaka, Japan) and the endotoxin levels were determined by Toxicolor® (Seikagaku Corp., Tokyo, Japan) as less than 1 EU/mg. K3 CpG ODN was synthesized by GeneDesign as previously described [48]. CFSE was purchased from Life Technologies (Carlsbad, CA, USA).

Immunizations and spleen cell cultures

After anesthetization, C57BL/6J mice were i.m. immunized with OVA (10 μg), or OVA and K3 CpG (10 μg), DMXAA (50 μg), c-di-GMP (1 μg), 2′3′ or 3′3′ cGAMP (1 μg), or K3 CpG + 2′3′/3′3′cGAMP/c-di-GMP/DMXAA at days 0 and 10. On day 17, OVA-specific serum IgG1 and IgG2c were measured by ELISA as

previously described [49]. The secondary antibodies used in IgG2c and IgG1 ELISAs were horseradish peroxidase conjugated goat anti-mouse IgG2c and IgG1 (Bethyl Laboratories, Montgomery, TX). On day 17, spleen cells were collected and single cell suspensions were prepared using a gentleMACS dissociator (Miltenyi Biotech, Gladbach, Germany). After red blood cell lysis using Tris-NH_4Cl buffer, cells were cultured in RPMI (containing 1% penicillin/streptomycin and 10% fetal calf serum [FCS)] and stimulated with total OVA (10 μg/mL) or OVA peptides (10 μg/mL) that are specific for MHC class I (OVA 257) or MHC class II (OVA 323) for 48 h. Production of IFN-γ and IL-13 were measured by ELISA.

hPBMC isolation and stimulation

All hPBMC experiments were conducted following approval from the Institutional Review Board of the National Institute of Biomedical Innovation. hPBMCs were isolated from the blood of healthy volunteer blood donors using human lymphocyte separation medium (IBL, Japan), and 1×10^6 cells were cultured in RPMI. PBMCs were stimulated with K3 CpG (10 μg/mL), cGAMP (10 μM), or K3 CpG + cGAMP for 24 h and production of IFN-γ and IL-12 were measured by ELISA.

For in vitro neutralization experiments, hPBMCs that were cultured as described above were subjected to IL-12/23p40 (clone: C8.6, BioLegend, San Diego, CA, USA), type-I IFN (clone: MMHAR-2, PBL Interferon Source, Piscataway, NJ, USA), or both IL-12/23p40 and type-I IFN neutralizing antibody treatments (5 μg/mL) 30 min before 24 h of stimulation.

mPBMC and DC cultures

mPBMCs were isolated from C57BL/6J mice using mouse lymphocyte separation medium (IBL, Japan), and 0.5×10^6 cells were cultured in RPMI. GM-DC cultures were prepared by flushing BM cells from the tibia and femurs of C57BL/6J mice and culturing these cells for 7 days in the presence of 20 ng/mL of GM-CSF (PeproTech, Rocky Hill, NJ, USA). GM-DCs were cultured in RPMI, containing 1% penicillin/streptomycin and 20% FCS. FL-DC cultures were prepared from BM cells of C57BL/6J mice that were cultured for 7 days in the presence of 100 ng/mL of human Flt3L (PeproTech). FL-DCs were cultured in RPMI, containing 1% penicillin/streptomycin and 10% FCS.

In vitro cytotoxicity assay

Splenocytes were isolated from C57BL/6J mice and 1×10^6 cells were cultured in RPMI in 96-well round-bottom plates for 24 h with the stimulants. After the stimulation, in order to prepare a positive control, Triton X-100 was added into the nonstimulated cells that were incubated at 37°C for 15 min. After centrifugation, supernatants of the cells were mixed with the substrate mix and incubated for 15 min at room temperature. ODs at 490 nm were measured and the percent cytotoxicity was calculated according to the instructions of the Non-Radioactive Cytotoxicity Assay Kit (Promega, WI, USA).

Cytokine measurement

Mouse IL-12p40, mouse IL-13, human IFN-γ, and human IL-12 levels were measured using ELISA kits from R&D Systems (Minneapolis, MN, USA). Mouse IFN-γ levels were determined using an ELISA kit from BioLegend.

Staining for intracellular cytokine and cell surface molecules

hPBMCs were stimulated with K3 CpG (10 μg/mL), cGAMP (10 μM), or K3 CpG + cGAMP for 16 h, with the last 4 h being in the presence of Brefeldin A. After the stimulation, cells were harvested and stained for surface molecules with CD16-PerCP-Cy5.5 (BD Biosciences, Franklin Lake, NJ), CD56-BV421 (BioLegend), CD3-FITC (BD Biosciences), and CD8-PE (Miltenyi Biotech) antibodies. Fixed and permeabilized cells were stained with IFN-γ-allophycocyanin (BioLegend) for the detection of intracellular IFN-γ and analyzed using the BD FACSCANTO II flow cytometer.

In vivo CTL cytotoxicity assay

Six-week-old C57BL/6J mice were immunized with OVA (10 μg) only, or OVA and either K3 CpG (10 μg), cGAMP (1 μg), or K3 + cGAMP once, via the i.m. route. On day 7, splenocytes from the naïve C57BL/6J mice were labeled with 2 or 0.2 μM of CFSE for 10 min at 37°C. The cells, which were labeled with 2 μM of CFSE, were subjected to peptide pulsing by incubating them with the OVA257 (10 μg/mL) for 90 min at 37°C. Then, the cells were washed, and equal numbers from each cells were transferred to the immunized mice via the i.v. route. Splenocytes were isolated, and upon staining with the LIVE/DEAD® Fixable Near-IR Dead Cell Stain (Invitrogen, Carlsbad, CA, USA), CFSE-labeled cells were analyzed by flow cytometry 24 h after the transfer.

Tumor cells and treatment

EG-7-OVA thymoma cells were purchased from American Type Culture Collection (VA, USA) and cultured in RPMI. A total of 1×10^6 cells were s.c. injected to the back of mice on day 0. On days 7 and 10, mice were given intratumor injections of PBS (50 μL), K3 CpG (10 μg), cGAMP (10 μg), or K3 CpG + cGAMP, and mice were monitored for tumor growth for 22 days.

B16 F10 melanoma cells were purchased from RIKEN Cell Bank (Japan) and cultured in DMEM. A total of 0.5×10^6 cells were s.c. injected to the back of mice on day 0. On days 8, 11, and 13, mice

were given intratumor injections of PBS (50 μL), K3 CpG (10 μg), cGAMP (10 μg), or K3 CpG + cGAMP, and mice were monitored for tumor growth for 17 days.

Statistical analysis

Mann–Whitney *U*-test, Student's *t*-test, or one-way ANOVA with Bonferroni's multiple comparison test were used for the statistical analyses ($*p < 0.05$; $**p < 0.01$; $***p < 0.001$). Statistical analyses were performed using GraphPad Prism software (La Jolla, CA, USA).

Acknowledgments: We thank Dr. Cevayir Coban for her comments and critical reading of the manuscript. We also thank the staff of the Animal Resource Center for Infectious Diseases (IFReC and RIMD, Osaka University) for their support in these studies and Prof. Akira's group for providing us the use of their flow cytometer. This study was supported in part by the Adjuvant Database Grant. E.K. received a grant-in aid for scientific research from the Ministry of Education, Culture, Sports, Science and Technology (MEXT) of Japan (grant number 24591145) and Takeda Science Foundation. E.K. was also supported by the Regional Strategy Support Program. B.T. received support in the form of a Japanese Government Scholarship from MEXT.

Conflict of interest: The authors declare no commercial or financial conflict of interest.

References

1 Kawai, T. and Akira, S., Review Toll-like receptors and their crosstalk with other innate receptors in infection and immunity. *Immunity* 2011. 34: 637–650.

2 Trinchieri, G. and Sher, A., Cooperation of Toll-like receptor signals in innate immune defence. *Nat. Rev. Immunol.* 2007. 7: 179–190.

3 Seder, R. A., Gazzinelli, R., Sher, A. and Paul, W. E., Interleukin 12 acts directly on CD4+ T cells to enhance priming for interferon gamma production and diminishes interleukin 4 inhibition of such priming. *Proc. Natl. Acad. Sci. USA* 1993. 90: 10188–10192.

4 Hsieh, C., Macatonia, S. E., Tripp, C. S., Wolf S. F., Garra A. O. and Murphy, K. M., Development of TH1 CD4+ T cells through IL-1 2 produced by Listeria-induced macrophages. *Science* 1993. 260: 547–549.

5 Spellberg, B. and Edwards, J. E., Type 1/type 2 immunity in infectious diseases. *Clin. Infect. Dis.* 2001. 90509: 76–102.

6 Mantovani, A. and Sica, A., Macrophages, innate immunity and cancer: balance, tolerance, and diversity. *Curr. Opin. Immunol.* 2010. 22: 231–237.

7 Hung, K., Hayashi, R., Lafond-Walker, A., Lowenstein, C., Pardoll, D. and Levitsky, H., The central role of CD4+ T cells in the antitumor immune response. *J. Exp. Med.* 1998. 188: 2357–2368.

8 Vesely, M. D., Kershaw, M. H., Schreiber, R. D. and Smyth, M. J., Natural innate and adaptive immunity to cancer. *Annu. Rev. Immunol.* 2011. 29: 235–271.

9 Vitale, M., Cantoni, C. and Pietra, G., Mingari, M. C. and Moretta, L., Effect of tumor cells and tumor microenvironment on NK-cell function. *Eur. J. Immunol.* 2014. 44: 1582–1592.

10 Hartmann, G. and Krieg, A. M., Mechanism and function of a newly identified CpG DNA motif in human primary B cells. *J. Immunol.* 2000. 164: 944–953.

11 Wagner, H., The immunobiology of the TLR9 subfamily. *Trends Immunol.* 2004. 25: 1–6.

12 Krieg, A. M., Therapeutic potential of Toll-like receptor 9 activation. *Nat. Rev. Drug Discov.* 2006. 5: 471–484.

13 Klinman, D. M., Immunotherapeutic uses of CpG oligodeoxynucleotides. *Nat. Rev. Immunol.* 2004. 4: 1–10.

14 Desmet, C. J. and Ishii, K. J., Nucleic acid sensing at the interface between innate and adaptive immunity in vaccination. *Nat. Rev. Immunol.* 2012. 12: 479–491.

15 Barber, G. N., Cytoplasmic DNA innate immune pathways. *Immunol. Rev.* 2011. 243: 99–108.

16 Sun, L., Wu, J., Du, F., Chen, X. and Chen, Z. J., Cyclic GMP-AMP synthase is a cytosolic DNA sensor that activates the type I interferon pathway. *Science* 2013. 339: 786–791.

17 Wu, J., Sun, L., Chen, X., Du, F., Shi, H., Chen, C. and Chen, Z. J., Cyclic GMP-AMP is an endogenous second messenger in innate immune signaling by cytosolic DNA. *Science* 2013. 339: 826–830.

18 Zhang, X., Shi, H., Wu, J., Zhang, X., Sun, L., Chen, C. and Chen, Z. J., Cyclic GMP-AMP containing mixed phosphodiester linkages is an endogenous high-affinity ligand for STING. *Mol. Cell.* 2013. 51: 226–235.

19 Burdette, D. L., Monroe, K. M., Sotelo-Troha, K., Iwig, J. S., Eckert, B., Hyodo, M., Hayakawa, Y. et al., STING is a direct innate immune sensor of cyclic di-GMP. *Nature* 2011. 478: 515–518.

20 Mcwhirter, S. M., Barbalat, R., Monroe, K. M., Fontana, M. F., Hyodo, M., Joncker, N. T., Ishii, K. J. et al., A host type I interferon response is induced by cytosolic sensing of the bacterial second messenger cyclic-di-GMP. *J. Exp. Med.* 2009. 206: 1899–1911.

21 Li, X. D., Wu, J., Gao, D., Wang, H., Sun, L. and Chen, Z. J., Pivotal roles of cGAS-cGAMP signaling in antiviral defense and immune adjuvant effects. *Science* 2013. 341: 1390–1394.

22 Tang, C. K., Aoshi, T., Jounai, N., Ito, J., Ohata, K., Kobiyama, K., Dessailly, B. H. et al., The chemotherapeutic agent DMXAA as a unique IRF3-dependent type-2 vaccine adjuvant. *PLoS One* 2013. 8: 1–6.

23 Hogenesch, H., Mechanism of immunopotentiation and safety of aluminum adjuvants. *Front. Immunol.* 2013. 3: 1–13.

24 Macleod, M. K. L., Mckee, A. S., David, A., Wang, J., Mason R. and Kappler, J. W., Vaccine adjuvants aluminum and monophosphoryl lipid A provide distinct signals to generate protective cytotoxic memory CD8 T cells. *Proc. Natl. Acad. Sci. USA* 2011. 108: 7914–7919.

25 Weeratna, R. D., Mccluskie, M. J., Xu, Y. and Davis, H. L., CpG DNA induces stronger immune responses with less toxicity than other adjuvants. *Vaccine* 2000. 18: 1755–1762.

26 Verthelyi, D., Ishii, K. J., Gursel, M., Takeshita, F. and Klinman, D. M., Human peripheral blood cells differentially recognize and respond to two distinct CpG Motifs. *J. Immunol.* 2001. 166: 2372–2377.

27 Hunter, A., Gabriel, K. E., Radzanowski, T., Neyer, L. E. and Remington, J. S., Type I interferons enhance production of IFN-γ by NK cells. *Immunol. Lett.* 1997. 59: 1–5.

28 Nguyen, K. B., Salazar-Mather, T. P., Dalod, M. Y., Van Deusen, J. B., Wei X. Q., Liew, F. Y., Caligiuri, M. A. et al., Coordinated and distinct roles for IFN-, IL-12, and IL-15 regulation of NK cell responses to viral infection. *J. Immunol.* 2002. 169: 4279–4287.

29 Kawai, T., Sato, S., Ishii, K. J., Coban, C., Hemmi, H., Yamamoto, M., Terai, K. et al., Interferon-alpha induction through Toll-like receptors involves a direct interaction of IRF7 with MyD88 and TRAF6. *Nat. Immunol.* 2004. 5: 1061–1068.

30 Chen, S., Kawashima, H., Lowe, J. B., Lanier, L. L. and Fukuda, M., Suppression of tumor formation in lymph nodes by L-selectin—mediated natural killer cell recruitment. *J. Exp. Med.* 2005. 202: 1679–1689.

31 Dubensky, T. W., Kanne, D. B. and Leong, M. L., Advances in vaccines rationale, progress and development of vaccines utilizing STING-activating cyclic dinucleotide adjuvants. *Ther. Adv. Vaccines.* 2013. 1: 131–143.

32 Way, S. S., Havenar-Daughton, C., Kolumam, G. A., Orgun, N. N. and Murali-Krishna, K., IL-12 and Type-I IFN synergize for IFN- production by CD4 T cells, whereas neither are required for IFN- production by CD8 T cells after Listeria monocytogenes infection. *J. Immunol.* 2007. 178: 4498–4505.

33 Krummen, M., Balkow, S., Shen, L., Heinz, S., Loquai, C., Probst, H.-C. and Grabbe, S., Release of IL-12 by dendritic cells activated by TLR ligation is dependent on MyD88 signaling, whereas TRIF signaling is indispensable for TLR synergy. *J. Leukoc. Biol.* 2010. 88: 189–199.

34 Hornung, V., Rothenfusser, S., Britsch, S., Krug, A., Jahrsdorfer, B., Giese, T., Endres, S. et al., Quantitative expression of Toll-like receptor 1–10 mRNA in cellular subsets of human peripheral blood mononuclear cells and sensitivity to CpG oligodeoxynucleotides. *J. Immunol.* 2002. 168: 4531–4537.

35 Chace, J. H., Hooker, N. A., Mildenstein, K. L., Krieg, A. M. and Cowdery, J. S., Bacterial DNA-induced NK cell IFN-g production is dependent on macrophage secretion of IL-12. *Clin. Immunol. Immunopathol.* 1997. 84: 185–193.

36 Swanson, C. L., Wilson, T. J., Strauch, P., Colonna, M., Pelanda, R. and Torres, R. M., Type I IFN enhances follicular B cell contribution to the T cell-independent antibody response. *J. Exp. Med.* 2010. 207: 1485–1500.

37 Chu, B. R. S., Targoni, O. S., Krieg, A. M., Lehmann, P. V. and Harding, C. V., CpG oligodeoxynucleotides act as adjuvants that switch on T helper 1 (Th1) immunity. *J. Exp. Med.* 1997. 186: 1623–1631.

38 Muller, K. M., Jaunin, F., Masouyc, I., Saurat, J. and Hauser, C., Cells mediate IL-4-dependent local tissue inflammation. *J. Immunol.* 1993. 150: 5576–5584.

39 Seki, Y., Inoue, H., Nagata, N., Hayashi, K., Fukuyama, S., Komine, O., Hamano, S. et al., SOCS-3 regulates onset and maintenance of Th2- mediated allergic responses. *Nat. Med.* 2003 9: 1047–1054.

40 Lin, L., Gerth, A. J. and Peng, S. L., CpG DNA redirects class-switching towards "Th1-like" Ig isotype production via TLR9 and MyD88. *Eur. J. Immunol.* 2004. 34: 1483–1487.

41 Gracie J. A. and Bradley J. A., Interleukin-12 induces interferon-γ-dependent switching of IgG alloantibody subclass. *Eur. J. Immunol.* 1996. 26: 1217–1221.

42 Van de Wetering, D., de Paus, R. A., van Dissel, J. T. and van de Vosse, E., IL-23 modulates CD56+/CD3- NK cell and CD56+/CD3 +NK-like T cell function differentially from IL-12. *Int. Immunol.* 2009. 21: 145–153.

43 Lankford, C. S. R. and Frucht, D. M., A unique role for IL-23 in promoting cellular immunity. *J. Leukoc. Biol.* 2003. 73: 49–56.

44 Cho, H. J., Takabayashi, K., Cheng, P., Nguyen, M., Corr, M, Tuck, S and Raz, E., Immunostimulatory DNA-based vaccines induce cytotoxic lymphocyte activity by a T-helper cell-independent mechanism. *Nat. Biotechnol.* 2000. 18: 509–514.

45 De Titta, A., Ballester, M., Julier, Z., Nembrini, C., Jeanbart, L., van der Vlies, A. J., Swartz, M. A. et al., Nanoparticle conjugation of CpG enhances adjuvancy for cellular immunity and memory recall at low dose. *Proc. Natl. Acad. Sci. USA* 2013. 110: 19902–19907.

46 Sauer, J. D., Sotelo-Troha, K., von Moltke, J., Monroe, K. M., Rae, C. S., Brubaker, S. W., Hyodo, M. et al., The N-ethyl-N-nitrosourea-induced Goldenticket mouse mutant reveals an essential function of Sting in the in vivo interferon response to Listeria monocytogenes and cyclic dinucleotides. *Infect. Immun.* 2011. 79: 688–694.

47 Honda, K., Yanai, H., Negishi, H., Asagiri, M., Sato, M., Mizutani, T., Shimada, N. et al., IRF-7 is the master regulator of type-I interferon-dependent immune responses. *Nature.* 2005. 434: 772–777.

48 Kobiyama, K., Aoshi, T., Narita, H., Kuroda, E., Hayashi, M., Tetsutani, K., Koyama, S. et al., Nonagonistic dectin-1 ligand transforms CpG into a multitask nanoparticulate TLR9 agonist. *Proc. Natl. Acad. Sci. USA* 2014. 111:3086–3091.

49 Kuroda, E., Ishii, K. J., Uematsu, S., Ohata, K., Coban, C., Akira, S., Aritake, K. et al., Article silica crystals and aluminum salts regulate the production of prostaglandin in macrophages. *Immunity* 2011. 34: 514–526.

Abbreviations: cGAMP: cyclic GMP—AMP · FL-DC: Flt3L-derived DC · GM-DC: GM-CSF-derived dendritic cell · IFNAR: IFNα/β receptor · pDC: plasmacytoid DC · STING: Stimulator of IFN genes

Full correspondence: Prof. Ken J. Ishii, Laboratory of Vaccine Science, WPI Immunology Frontier Research Center (iFReC), Osaka University, Osaka 565-0871, Japan
Fax: +81-6-6879-4812
e-mail: kenishii@biken.osaka-u.ac.jp

Received: 14/8/2014
Revised: 3/11/2014
Accepted: 17/12/2014
Accepted article online: 22/12/2014

nature immunology

Perivascular leukocyte clusters are essential for efficient activation of effector T cells in the skin

Yohei Natsuaki[1,2,15], Gyohei Egawa[1,15], Satoshi Nakamizo[1], Sachiko Ono[1], Sho Hanakawa[1], Takaharu Okada[3], Nobuhiro Kusuba[1], Atsushi Otsuka[1], Akihiko Kitoh[1], Tetsuya Honda[1], Saeko Nakajima[1], Soken Tsuchiya[4], Yukihiko Sugimoto[4], Ken J Ishii[5,6], Hiroko Tsutsui[7], Hideo Yagita[8], Yoichiro Iwakura[9,10], Masato Kubo[11,12], Lai guan Ng[13], Takashi Hashimoto[2], Judilyn Fuentes[14], Emma Guttman-Yassky[14], Yoshiki Miyachi[1] & Kenji Kabashima[1]

It remains largely unclear how antigen-presenting cells (APCs) encounter effector or memory T cells efficiently in the periphery. Here we used a mouse contact hypersensitivity (CHS) model to show that upon epicutaneous antigen challenge, dendritic cells (DCs) formed clusters with effector T cells in dermal perivascular areas to promote *in situ* proliferation and activation of skin T cells in a manner dependent on antigen and the integrin LFA-1. We found that DCs accumulated in perivascular areas and that DC clustering was abrogated by depletion of macrophages. Treatment with interleukin 1α (IL-1α) induced production of the chemokine CXCL2 by dermal macrophages, and DC clustering was suppressed by blockade of either the receptor for IL-1 (IL-1R) or the receptor for CXCL2 (CXCR2). Our findings suggest that the dermal leukocyte cluster is an essential structure for elicitating acquired cutaneous immunity.

Boundary tissues, including the skin, are continually exposed to foreign antigens, which must be monitored and possibly eliminated. Upon exposure to foreign antigens, skin dendritic cells (DCs), including epidermal Langerhans cells (LCs), capture the antigens and migrate to draining lymph nodes (LNs), where the presentation of antigen to naive T cells occurs mainly in the T cell zone. In this location, the accumulation of naive T cells in the vicinity of DCs is mediated by signaling via the chemokine receptor CCR7 (ref. 1). The T cell zone in the draining LNs facilitates the efficient encounter of antigen-bearing DCs with antigen-specific naive T cells.

In contrast to T cells in LNs, the majority of T cells in the skin, including infiltrating skin T cells and skin-resident T cells, have an effector-memory phenotype[2]. In addition, the presentation of antigen to skin T cells by antigen-presenting cells (APCs) is the crucial step in the elicitation of acquired skin immune responses, such as contact dermatitis. Therefore, we investigated how antigen presentation occurs in the skin and if it is different from antigen presentation in LNs. Published studies using mouse contact hypersensitivity (CHS) as a model of human contact dermatitis have revealed that dermal DCs (dDCs) have a pivotal role in the transport and presentation of antigen to the LNs, but epidermal LCs do not[3]. In the skin, however, it remains unclear which subset of APCs presents antigens to skin T cells and how skin T cells efficiently encounter APCs. In addition, dermal macrophages are key modulators in CHS responses[4], but the precise mechanisms by which macrophages are involved in the recognition of antigen in the skin have not yet been clarified. These unanswered questions prompted us to investigate where skin T cells recognize antigens and how skin T cells are activated in the elicitation phase of acquired cutaneous immune responses such as CHS.

When keratinocytes encounter foreign antigens, they immediately produce various proinflammatory mediators, such as interleukin 1 (IL-1) and tumor-necrosis factor, in an antigen-nonspecific manner[5,6]. Proteins of the IL-1 family are considered important modulators in CHS responses because the activation of hapten-specific T cells is impaired in mice deficient in both IL-1α and IL-1β but not in mice deficient in tumor-necrosis factor[7]. IL-1α and IL-1β are agonistic ligands of the receptor for IL-1 (IL-1R). While IL-1α is stored in keratinocytes and is secreted upon exposure to nonspecific stimuli, IL-1β is produced mainly by epidermal LCs and dermal mast cells in an inflammasome-dependent manner via activation of the cytoplasmic pattern-recognition receptor NLRP3 and of caspase-1 and caspase-11. Because IL-1α and IL-1β are crucial in the initiation of acquired

[1]Department of Dermatology, Kyoto University Graduate School of Medicine, Kyoto, Japan. [2]Department of Dermatology, Kurume University School of Medicine, Fukuoka, Japan. [3]Research Unit for Immunodynamics, RIKEN Research Center for Allergy and Immunology, Kanagawa, Japan. [4]Department of Pharmaceutical Biochemistry, Graduate School of Pharmaceutical Sciences, Kumamoto University, Kumamoto, Japan. [5]Laboratory of Adjuvant Innovation, National Institute of Biomedical Innovation, Osaka, Japan. [6]Laboratory of Vaccine Science, WPI Immunology Frontier Research Center, Osaka University, Osaka, Japan. [7]Department of Microbiology, Hyogo College of Medicine, Hyogo, Japan. [8]Department of Immunology, Juntendo University School of Medicine, Tokyo, Japan. [9]Research Institute for Biomedical Sciences, Tokyo University of Science, Chiba, Japan. [10]Medical Mycology Research Center, Chiba University, Chiba, Japan. [11]Laboratory for Cytokine Regulation, RIKEN center for Integrative Medical Science, Kanagawa, Japan. [12]Division of Molecular Pathology, Research Institute for Biomedical Science, Tokyo University of Science, Chiba, Japan. [13]Singapore Immunology Network, Agency for Science, Technology and Research, Biopolis, Singapore. [14]Department of Dermatology, Icahn School of Medicine at Mount Sinai School Medical Center, New York, New York, USA. [15]These authors contributed equally to this work. Correspondence should be addressed to K.K. (kaba@kuhp.kyoto-u.ac.jp).

Received 7 July; accepted 19 August; published online 21 September 2014; doi:10.1038/ni.2992

immune responses such as CHS, it is of great interest to understand how IL-1 modulates the recognition of antigen by skin T cells.

Using a mouse CHS model, here we examined how DCs and effector T cells encounter each other efficiently in the skin. We found that upon encountering antigenic stimuli, dDCs formed clusters in which effector T cells were activated and proliferated in an antigen-dependent manner. These DC–T cell clusters were initiated by skin macrophages via IL-1R signaling and were essential for the establishment of cutaneous acquired immune responses.

RESULTS

Formation of DC–T cell clusters at antigen-challenged sites

To explore the accumulation of cells of the immune system in the skin, we examined the clinical and histological features of the elicitation of human allergic contact dermatitis. Allergic contact dermatitis is the most common of eczematous skin diseases, affecting 15–20% of the general population worldwide[8], and is mediated by T cells. Although antigens should be spread evenly over the surface of skin, clinical manifestations commonly include discretely distributed small vesicles (**Fig. 1a**), which suggests an uneven occurrence of intense inflammation. Histological examination of allergic contact dermatitis showed spongiosis, intercellular edema in the epidermis and colocalization of perivascular infiltrates of $CD3^+$ T cells and spotty accumulation of $CD11c^+$ DCs in the dermis, especially beneath the vesicles (**Fig. 1b**). These findings led us to hypothesize that focal accumulation of T cells and DCs in the dermis might contribute to vesicle formation in early eczema.

To characterize the DC–T cell clusters in elicitation reactions, we used two-photon microscopy to obtain time-lapse images in a mouse model of CHS. We isolated T cells from the draining LNs of mice sensitized with the hapten DNFB (2,4-dinitrofluorobenzene), labeled the cells with fluorescent dye and transferred them into mice that express the common DC marker CD11c tagged with yellow fluorescent protein (YFP). In the steady state, YFP^+ dDCs distributed diffusely (**Fig. 1c**), representative of nondirected movement in a random fashion (**Supplementary Fig. 1**), as reported before[9]. After topical challenge with DNFB, YFP^+ dDCs transiently increased their velocity and formed clusters in the dermis, with the clusters becoming larger and more evident after 24 h (**Fig. 1c** and **Supplementary Movie 1**). At the same time, transferred T cells accumulated in the DC clusters and interacted with YFP^+ DCs for several hours (**Fig. 1d** and **Supplementary Movie 2**). Thus, we observed accumulation of DCs and T cells in the dermis in mice during CHS responses. We noted that the intercellular spaces between keratinocytes overlying the DC–T cell clusters in the dermis were enlarged (**Fig. 1e**), which replicated observations made for human allergic contact dermatitis (**Fig. 1b**).

We next sought to determine which of the two main DC populations in skin, epidermal LCs or dDCs, was essential for the elicitation of CHS. To deplete mice of all cutaneous DC subsets, we used mice with sequence expressing the diphtheria toxin receptor (DTR) under the control of the promoter of the gene encoding langerin as recipients (in such 'Langerin-DTR' mice, treatment with diphtheria toxin (DT) leads to depletion of langerin-positive cells) and mice that express a transgene encoding DTR under the control of promoter of the gene encoding CD11c as donors (in such 'CD11c-DTR' mice, treatment with DT leads to transient depletion of $CD11c^+$ DC populations). To selectively deplete mice of LCs or dDCs, we transferred bone marrow (BM) cells from C57BL/6 mice or CD11c-DTR mice into Langerin-DTR or C57BL/6 mice, respectively (**Supplementary Fig. 2a,b**). We injected DT into the chimeras to ensure depletion of each DC subset before elicitation and found that ear swelling and inflammatory histological findings were significantly attenuated in the absence of dDCs but not in the absence of LCs (**Fig. 1f** and **Supplementary Fig. 2c**). In addition, production of interferon-γ (IFN-γ) in skin T cells was substantially suppressed in mice depleted of dDCs (**Fig. 1g**). These results suggested that dDCs, not epidermal LCs, were essential for T cell activation and the elicitation of CHS responses.

Antigen-dependent proliferation of skin effector T cells *in situ*

To evaluate the effect of DC–T cell clusters in the dermis, we determined whether T cells had acquired the ability to proliferate via the accumulation of DC–T cell clusters in the dermis. We purified $CD4^+$ or $CD8^+$ T cells from the draining LNs of DNFB-sensitized mice, labeled

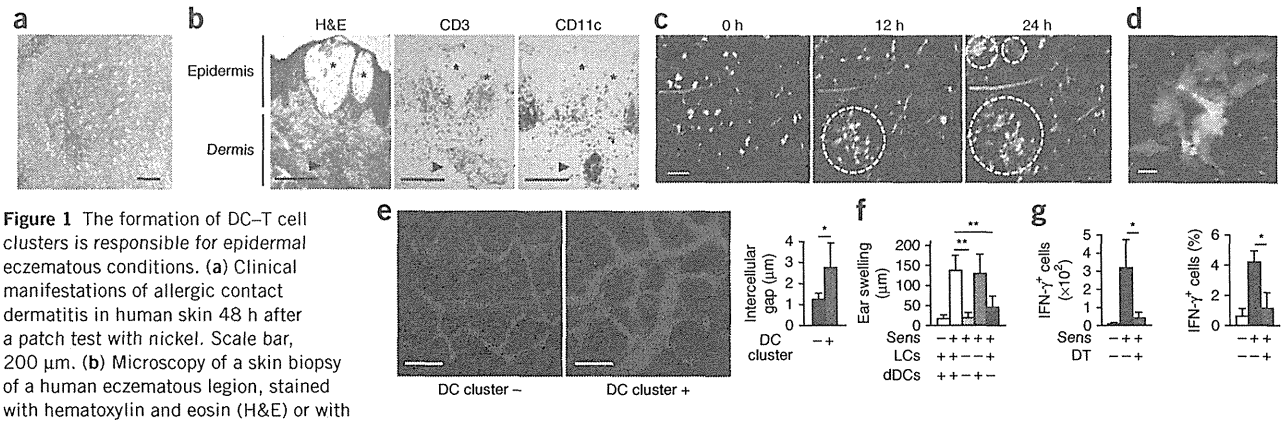

Figure 1 The formation of DC–T cell clusters is responsible for epidermal eczematous conditions. (**a**) Clinical manifestations of allergic contact dermatitis in human skin 48 h after a patch test with nickel. Scale bar, 200 μm. (**b**) Microscopy of a skin biopsy of a human eczematous legion, stained with hematoxylin and eosin (H&E) or with antibody to CD3 (anti-CD3) or anti-CD11c. *, epidermal vesicles; arrowheads indicate dDC–T cell clusters. Scale bars, 250 μm. (**c**) Sequential images of leukocyte clusters in the elicitation phase of CHS. White outlined areas indicate dermal accumulation of DCs (green) and T cells (red). Scale bar, 100 μm. (**d**) Enlargement of DC–T cell cluster in **c**. Scale bar,10 μm. (**e**) Intercellular edema of the epidermis overlying a DC–T cell cluster in the dermis, with keratinocytes (red) visualized with isolectin B4 (left), and distance between adjacent keratinocytes above (+) or not above (–) a DC–T cell cluster ($n = 20$ images per condition) (right). Scale bars, 10 μm. (**f**) Ear swelling 24 h after CHS with (+) or without (–) sensitization (Sens) and with (–) or without (+) subset-specific depletion of DCs ($n = 5$ mice per group). (**g**) Quantification (left) and frequency (right) of IFN-γ-producing T cells in the ear 18 h after CHS with or without sensitization (as in **f**) and with (DT +) or without (DT –) depletion of dDCs ($n = 5$ mice per group). $^*P < 0.05$ and $^{**}P < 0.001$ (unpaired Student's *t*-test). Data are representative of five independent experiments (**a–d**) or three experiments (**f,g**) or are pooled from three experiments (**e**; error bars (**e–g**), s.d.).

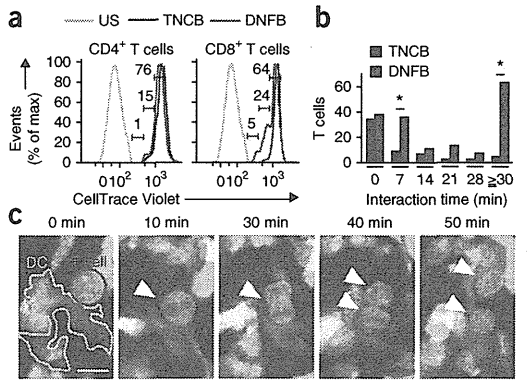

Figure 2 Antigen-dependent T cell proliferation in DC–T cell clusters. (**a**) Proliferation $CD4^+$ T cells (left) or $CD8^+$ T cells (right) in the skin of recipient mice 24 h after transfer of CellTrace Violet–labeled cells from donor mice left unsensitized (US) or sensitized with DNFB or TNCB, assessed as dilution of tracer in the challenged sites. Numbers adjacent to bracketed lines indicate percent cells that had proliferated. (**b**) Conjugation time of dDCs with T cells sensitized with DNFB ($n = 160$ T cells) or TNCB ($n = 60$ T cells), assessed at 24 h after challenge with DNFB. $^*P < 0.05$ (unpaired Student's *t*-test). (**c**) Sequential images of dividing T cells (red) in DC–T cell clusters. Green, dDCs; arrowheads indicate a dividing T cell. Data are representative of three experiments.

the cells with a division-tracking dye and transferred the cells into naive mice. Twenty-four hours after the application of DNFB to the recipient mice, we collected the skin to evaluate T cell proliferation by dilution of fluorescence intensity. Most of the infiltrating T cells (>90%) were $CD44^+CD62L^-$ effector T cells (**Supplementary Fig. 2d**). Among the infiltrating T cells, $CD8^+$ T cells proliferated actively, whereas the $CD4^+$ T cells showed low proliferative potency (**Fig. 2a**). This T cell proliferation was antigen dependent because T cells sensitized with the hapten TNCB (2,4,6-trinitrochlorobenzene) exhibited low proliferative activity in response to the application of DNFB (**Fig. 2a**). In line with that finding, the DC–T cell conjugation time was prolonged in the presence of the cognate antigen DNFB (**Fig. 2b**), and the T cells interacting with DCs within DC–T cell clusters proliferated (**Fig. 2c** and **Supplementary Movie 3**). These findings indicated that skin effector T cells conjugated with DCs and proliferated *in situ* in an antigen-dependent manner.

LFA-1-dependent activation of $CD8^+$ T cells in DC–T cell clusters

Sustained interaction between DCs and naive T cells, known as the 'immunological synapse', is maintained by cell adhesion molecules[10]. In particular, the integrin LFA-1 (CD58) on T cells binds to cell-surface glycoproteins, such as the intercellular adhesion molecule ICAM-1, on APCs, which is essential for the proliferation and activation of naive T cells during antigen recognition in the LNs. To determine whether LFA-1–ICAM-1 interactions are required for the activation of effector T cells in DC–T cell clusters in the skin, we elicited a CHS response in mouse ear skin with DNFB, then injected KBA, a neutralizing antibody to LFA-1, intravenously 14 h later. Such administration of KBA reduced the accumulation of T cells in the dermis (**Fig. 3a**). The velocity of T cells in the cluster was 0.65 ± 0.29 μm/min (mean ± s.d.) at 14 h after the DNFB challenge and increased up to threefold (1.64 ± 1.54 μm/min) at 8 h after treatment with KBA, while it was not affected by treatment with the isotype-matched control antibody immunoglobulin G (IgG) (**Fig. 3b**). At the outside of clusters, T cells smoothly migrated at the mean velocity of 2.95 ± 1.19 μm/min, consistent with published results[11], and this was not affected by treatment with the control antibody IgG (data not shown). Treatment with KBA also significantly attenuated ear swelling (**Fig. 3c**) as well as IFN-γ production by skin $CD8^+$ T cells (**Fig. 3d,e**). These results suggested that the DC–effector T cell conjugates were integrin dependent, similar to the DC–naive T cell interactions in draining LNs.

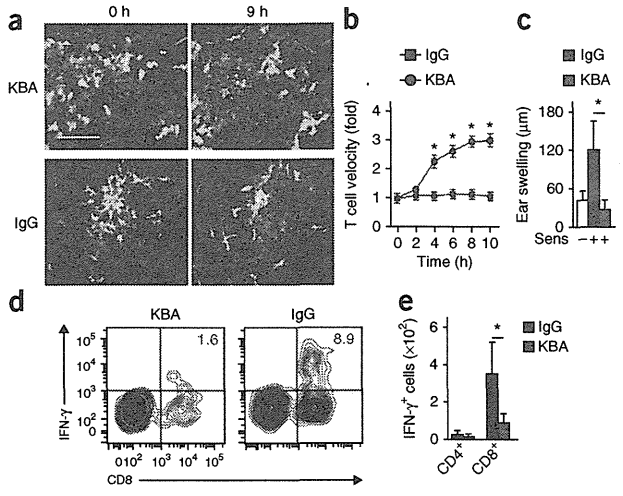

Figure 3 LFA-1 is essential for the persistence of DC–T cell clustering and for T cell activation in the skin. (**a**) Clusters of DCs (green) and T cells (red) in the DNFB-challenged site before (0 h) and 9 h after treatment with KBA (LFA-1-neutralizing antibody) or IgG (isotype-matched control antibody). Scale bar, 100 μm. (**b**) T cell velocity in DNFB-challenged sites at various times (horizontal axis) after treatment with KBA or IgG ($n = 30$ T cells per group), presented relative to velocity at time 0, set as 1. (**c**) Ear swelling 24 h after treatment with KBA or IgG in mice ($n = 5$ per group) left unsensitized (Sens –) or challenged with DNFB (Sens +). (**d,e**) IFN-γ production by $CD8^+$ T cells (**d**) and quantification of IFN-γ-producing cells in the $CD4^+$ or $CD8^+$ population (**e**) in skin from mice ($n = 5$ per group) challenged with DNFB, then treated with KBA or IgG 12 h later, assessed 6 h after antibody treatment. Numbers in top right quadrants (**d**) indicate percent IFN-γ^+CD8^+ T cells. $^*P < 0.05$ (unpaired Student's *t*-test). Data are representative of three experiments (error bars (**b,c,e**), s.d.).

dDC clustering requires skin macrophages

We next examined the factors that initiated the accumulation of DC–T cell clusters. dDC clusters also formed in response to the initial application of hapten (sensitization phase), but their number decreased significantly 48 h after sensitization, while DC clusters persisted for 48 h in the elicitation phase (**Fig. 4a** and **Supplementary Fig. 3a**). These DC clusters were abrogated 7 d after application of DNFB (data not shown). These observations suggested that the accumulation of DC–T cell clusters was initiated by DC clustering, which then induced the accumulation, proliferation and activation of T cells, a process that depended on the presence of antigen-specific effector T cells *in situ*. DC clusters were also induced by solvents (such as acetone) or adjuvants (such as dibutylphthalic acid) and by pathogenic inoculation with *Mycobacterium bovis* bacillus Calmette-Guérin (**Supplementary Fig. 3b,c**). In addition, we observed DC clusters not only in the ear skin but also in other regions, such as the back skin and the footpad (**Supplementary Fig. 3d**). These results suggested that the formation of DC clusters was not an ear-specific event but was a general mechanism during skin inflammation.

The abundance of DC clusters in response to the application of DNFB was not altered in mice that lack T cells and B cells (recombinase

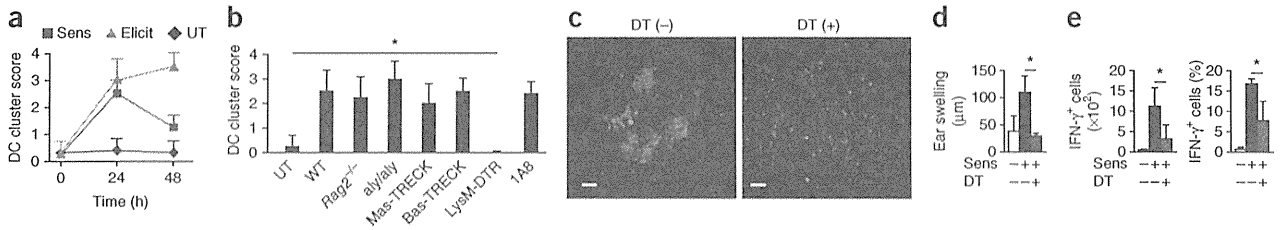

Figure 4 Macrophages are essential for DC cluster formation. (**a**) Score of DC cluster abundance in mice ($n = 4$ per group) left untreated (UT) or 24 h and 48 h after application of DNFB in the sensitization or elicitation phase of CHS; scores were assigned according to the size and number of clusters. (**b**) Score of DC cluster abundance (as in **a**) in untreated wild-type mice (UT), in DNFB-treated wild-type (C57BL/6) mice (WT), RAG-2-deficient mice (*Rag2*$^{-/-}$), aly/aly mice (aly/aly), DT-treated Mas-TRECK or Bas-TRECK mice or DT-treated C57BL/6 recipients of LysM-DTR BM cells, and in wild-type mice treated with 1A8 (anti-Ly6G) ($n = 4$ mice per group). (**c**) DC clusters in C57BL/6 chimeras given LysM-DTR BM with (right) or without (left) treatment of recipients with DT. Scale bars, 100 μm. (**d**) Ear swelling in C57BL/6 chimeras ($n = 5$ per group) given LysM-DTR BM with or without treatment with DT, assessed 24 h after no DNFB (Sense −) or application of DNFB to the recipients. (**e**) Quantification (left) and frequency (right) of IFN-γ-producing CD8$^+$ T cells in mice as in **d** ($n = 5$ per group). $^*P < 0.05$ (unpaired Student's *t*-test). Data are representative of three (**a**,**c**,**e**), two (**b**) or four (**d**) experiments (error bars (**b**,**d**,**e**), s.d.).

RAG-2–deficient mice), in mice deficient in lymphoid tissue–inducer cells (alymphoblastic (aly/aly) mice)[12] or in mice depleted of mast cells or basophils (Mas-TRECK or Bas-TRECK mice treated with DT)[13,14] (**Fig. 4b**). In contrast, DC clustering was abrogated in C57BL/6 mice given transfer of BM from LysM-DTR mice (with sequence encoding a DTR cassette inserted into the gene encoding lysozyme M) followed by treatment of the recipients with DT to ensure depletion of both macrophages and neutrophils (**Fig. 4b,c**). Depletion of neutrophils alone, by administration of antibody 1A8 to Ly6G, did not interfere with the formation of DC clusters (**Fig. 4b**), which suggested that macrophages were required during the formation of DC clusters, but neutrophils were not. Of note, the formation of DC clusters was not attenuated by treatment with the LFA-1-neutralizing antibody KBA (**Supplementary Fig. 3e,f**), which suggested that macrophage-DC interactions were LFA-1 independent. Consistent with the formation of DC clusters, elicitation of the CHS response (**Fig. 4d**) and IFN-γ production by skin T cells (**Fig. 4e**) were significantly suppressed in chimeras given LysM-DTR BM and treated with DT. Thus, skin macrophages were required for the formation of DC clusters, which was necessary for T cell activation and the elicitation of CHS.

Perivascular DCs clustering requires macrophages

To examine the migratory kinetics of dermal macrophages and DCs *in vivo*, we visualized them by two-photon microscopy. *In vivo* labeling of blood vessels with dextran conjugated to the hydrophobic red fluorescent dye TRITC (tetramethylrhodamine isothiocyanate) revealed that dDCs distributed diffusely in the steady state (**Fig. 5a**, left). After application of DNFB to the ears of mice previously sensitized with DNFB, dDCs accumulated mainly around post-capillary venules (**Fig. 5a**, right, and **b**). Time-lapse imaging revealed that some dDCs showed directional migration toward TRITC$^+$ cells that were labeled red by incorporation of extravasated TRITC-dextran (**Fig. 5c** and **Supplementary Movie 4**). Most of the TRITC$^+$ cells were F4/80$^+$CD11b$^+$ macrophages (**Supplementary Fig. 4a**). These observations prompted us to investigate the role of macrophages in DC accumulation. We used a chemotaxis assay to determine whether macrophages attracted the DCs. We isolated dDCs and dermal macrophages from dermal skin cell suspensions and incubated them for 12 h in a Transwell assay. dDCs placed in the upper wells migrated efficiently to lower wells that contained dermal macrophages (**Fig. 5d**). However, we did not observe such dDC migration when macrophages were absent from the lower wells (**Fig. 5d**). Thus, dermal macrophages were able to attract dDCs *in vitro*, which may have led to the accumulation of dDCs around post-capillary venules.

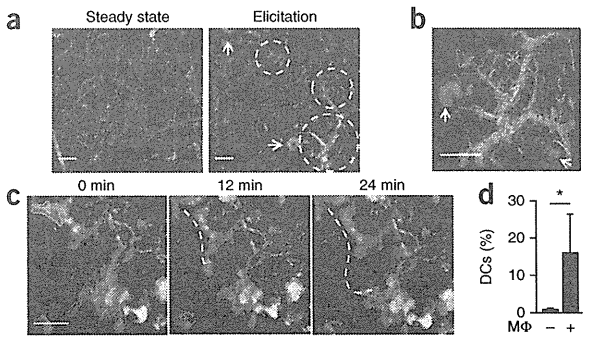

Figure 5 Macrophages mediate the perivascular formation of DC clusters. (**a**) Distribution of dDCs (green) in the steady state (left) and in the elicitation phase of CHS (right). White outlined areas indicate DC clusters; arrows indicate sebaceous glands visualized with BODIPY (green); yellow and red, blood vessels; red, macrophages. Scale bars, 100 μm. (**b**) Enlargement of a perivascular DC cluster. Arrows indicate sebaceous glands of hair follicles. Scale bar, 100 μm.(**c**) Sequential images of dDCs (green) and macrophages (red) in the elicitation phase of CHS. White dashed line represents the track of a DC. Scale bar, 30 μm. (**d**) Chemotaxis of dDCs in the presence (+) or absence (−) of macrophages (MΦ) prepared from ear skin, presented as the frequency of dDCs that transmigrated into the lower chamber of a Transwell (relative to input dDCs). $^*P < 0.05$ (unpaired Student's *t*-test). Data are representative of three experiments (error bars (**d**), s.d.).

DC cluster formation requires IL-1α upon antigen challenge

We attempted to explore the mechanism underlying the formation of DC clusters. We observed that DC accumulation occurred during the first application of hapten (**Fig. 4a**), which suggested that an antigen-nonspecific mechanism, such as production of the proinflammatory mediator IL-1, may initiate DC clustering. DNFB-induced accumulation of DCs was not suppressed in mice deficient in NLRP3 or deficient in caspase-1 and caspase-11 more than their wild-type counterparts, but it was significantly lower in IL-1R1-deficient mice (which lack the receptor for IL-1α and IL-1β and for the IL-1 receptor antagonist (IL-1ra)) than in their wild-type counterparts, as well as after the subcutaneous administration of IL-1ra than before treatment with the antagonist (**Fig. 6a,b**). Consistent with those observations, the elicitation of CHS and IFN-γ production by skin T cells were significantly attenuated in mice that lacked both IL-1α and IL-1β (**Fig. 6c,d**). In addition, the formation of dDC clusters was suppressed significantly by the subcutaneous injection of a neutralizing antibody to IL-1α but

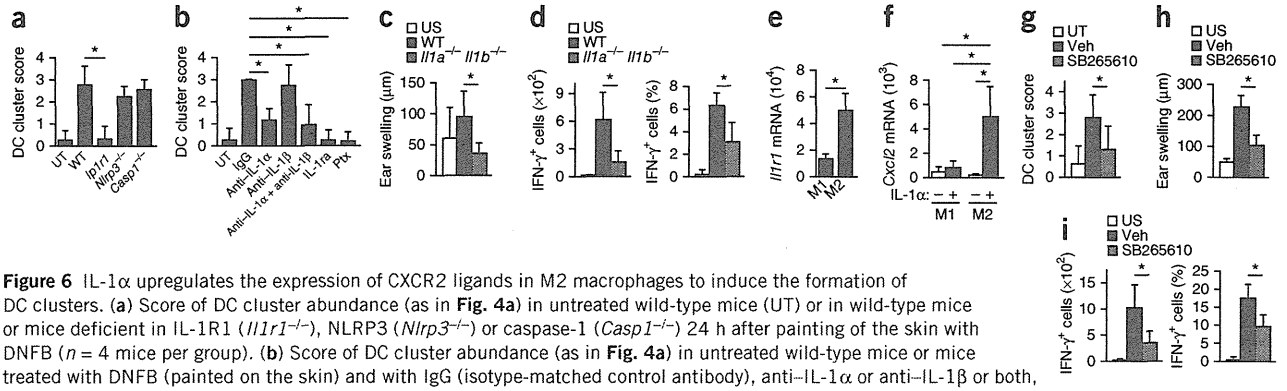

Figure 6 IL-1α upregulates the expression of CXCR2 ligands in M2 macrophages to induce the formation of DC clusters. (**a**) Score of DC cluster abundance (as in **Fig. 4a**) in untreated wild-type mice (UT) or in wild-type mice or mice deficient in IL-1R1 (*Il1r1*$^{-/-}$), NLRP3 (*Nlrp3*$^{-/-}$) or caspase-1 (*Casp1*$^{-/-}$) 24 h after painting of the skin with DNFB ($n = 4$ mice per group). (**b**) Score of DC cluster abundance (as in **Fig. 4a**) in untreated wild-type mice or mice treated with DNFB (painted on the skin) and with IgG (isotype-matched control antibody), anti–IL-1α or anti–IL-1β or both, recombinant IL-1ra or pertussis toxin (Ptx), assessed 24 h after treatment with hapten ($n = 4$ mice per group). (**c**,**d**) Ear swelling 24 h after application of DNFB (**c**) and quantification (**d**, left) and frequency (**d**, right) of IFN-γ-producing CD8$^+$ T cells in the ear 18 h after application of DNFB (**d**) in unsensitized wild-type mice (US) or in mice lacking both IL-1α and IL-1β (*Il1a*$^{-/-}$*Il1b*$^{-/-}$) and wild-type mice given adoptive transfer of DNFB-sensitized T cells ($n = 5$ mice per group). (**e**) Quantitative RT-PCR analysis of *Il1r1* mRNA in M1 or M2 macrophages ($n = 4$ mice per group). (**f**) Quantitative RT-PCR analysis of *Cxcl2* mRNA in M1 or M2 macrophages cultured with (+) or without (−) IL-1α. (**g**) Score of DC cluster abundance (as in **Fig. 4a**) in untreated wild-type mice (UT) or in mice treated with DNFB (painted on the skin) in the presence (SB265610) or absence (vehicle (Veh)) of a CXCR2 inhibitor, assessed 24 h after treatment with DNFB ($n = 4$ mice per group). (**h**,**i**) Ear swelling 24 h after application of DNFB (**h**) and quantification (**i**, right) and frequency (**i**, left) of IFN-γ-producing CD8$^+$ T cells 18 h after application of DNFB (**i**) in unsensitized wild-type mice (US) or in mice treated with DNFB in the presence or absence of the CXCR2 inhibitor SB265610 ($n = 5$ mice per group). *$P < 0.05$ (unpaired Student's *t*-test). Data are representative of two (**a**,**c**,**d**) or three (**b**,**e**–**i**) experiments (error bars, s.d.).

was suppressed only marginally by a neutralizing antibody to IL-1β (**Fig. 6b**). Because keratinocytes are known to produce IL-1α upon application of a hapten[15], our results suggested a major role for IL-1α in mediating the formation of DC clustering.

M2 macrophages produce chemokine CXCL2 to attract dDCs

To further characterize how macrophages attract dDCs, we examined expression of the gene encoding IL-1Rα (*Il1r1*) in BM-derived classically activated (M1) and alternatively activated (M2) macrophages, classified as such on the basis of differences in the expression of *Tnf*, *Nos2*, *Il12a*, *Arg1*, *Retnla* and *Chi313* mRNA[16] (**Supplementary Fig. 4b**). We found that M2 macrophages had higher expression of *Il1r1* mRNA than did M1 macrophages (**Fig. 6e**). We also found that subcutaneous injection of pertussis toxin, an inhibitor specific for inhibitory regulative G protein, almost completely abrogated the formation of DC clusters in response to hapten stimuli (**Fig. 6b**), which suggested that signaling through chemokines coupled to the inhibitory regulative G protein was required for the formation of DC clusters.

We next used microarray analysis to examine the effect of IL-1α on the expression of chemokine-encoding genes in M1 and M2 macrophages. Treatment with IL-1α did not enhance such expression in M1 macrophages, whereas it increased the expression of *Ccl5*, *Ccl17*, *Ccl22* and *Cxcl2* mRNA in M2 macrophages (**Supplementary Table 1**). Among those, *Cxcl2* mRNA expression was enhanced most prominently by treatment with IL-1α, a result we confirmed by real-time PCR analysis (**Fig. 6f**). Consistently, *Cxcl2* mRNA expression was much higher in DNFB-painted skin than in untreated skin (**Supplementary Fig. 5a**) and was not affected by neutrophil depletion with the 1A8 antibody to Ly6G (**Supplementary Fig. 5b,c**). In addition, IL-1α-treated dermal macrophages produced *Cxcl2* mRNA *in vitro* (**Supplementary Fig. 5d**). These results suggested that dermal macrophages, but not neutrophils, were the main source of CXCL2 during CHS. We also detected high expression of *Cxcr2* mRNA (which encodes the receptor for CXCL2) in DCs (**Supplementary Fig. 5e**); this prompted us to examine the role of CXCR2 in dDCs. The formation of DC clusters in response to DNFB was substantially reduced by intraperitoneal administration of the CXCR2 inhibitor SB265610 (ref. 17) (**Fig. 6g**). In addition, treatment with SB265610 during the elicitation of CHS with DNFB inhibited ear swelling (**Fig. 6h**) and IFN-γ production by skin T cells (**Fig. 6i**).

Together our results indicated that in the absence of effector T cells specific for a cognate antigen (i.e., in the sensitization phase of CHS), DC clustering was a transient event, and hapten-carrying DCs migrated into draining LNs to establish sensitization. On the other hand, in the presence of the antigen and antigen-specific effector or memory T cells, DC clustering was followed by accumulation of T cells (i.e., in the elicitation phase of CHS) (**Supplementary Fig. 6**). Thus, dermal macrophages were essential for initiating the formation of DC clusters through the production of CXCL2, and DC clustering had a role in the efficient activation of skin T cells.

DISCUSSION

Although the mechanistic events in the sensitization phase in cutaneous immunity have been studied thoroughly over 20 years[18,19], the types of immunological events that occur during the elicitation phases in the skin has remained unclear. Here we have described the antigen-dependent induction of DC–T cell clusters in the skin in a mouse model of CHS and showed that DC–effector T cell interactions in these clusters were required for the induction of efficient antigen-specific immune responses in the skin. We found that dDCs, but not epidermal LCs, were essential for the presentation of antigen to skin effector T cells and that they exhibited sustained association with effector T cells in an antigen- and LFA-1-dependent manner. IL-1α, not the inflammasome, initiated the formation of these perivascular DC clusters.

Epidermal contact with antigens triggers the release of IL-1 in the skin[15]. Published studies have shown that the epidermal keratinocytes constitute a major reservoir of IL-1α[6] and that mechanical stress applied to keratinocytes permits the release of large amounts of IL-1α even in the absence of cell death[20]. The cellular source of IL-1α in this process remains unclear. We found that IL-1α activated macrophages that subsequently attracted dDCs, mainly to areas around post-capillary venules, where effector T cells are known to transmigrate from the blood into the skin[21]. In the presence of the antigen and antigen-specific

effector T cells, DC clustering was followed by T cell accumulation. Therefore, we propose that these perivascular dDC clusters may provide antigen-presentation sites for efficient activation of effector T cells. This is suggested by the observations that CHS responses and intracutaneous T cell activation were attenuated substantially in the absence of these clusters, in conditions of macrophage depletion or inhibition of integrin function, IL-1R signaling[22,23] or CXCR2 signaling[24].

In contrast to antigen presentation in the skin, antigen presentation in other peripheral barrier tissues is relatively well understood. In submucosal areas, specific sentinel lymphoid structures (mucosa-associated lymphoid tissue (MALT)) serve as peripheral antigen-presentation sites[25], and lymphoid follicles are present in non-inflammatory bronchi (bronchus-associated lymphoid tissue (BALT)). These structures serve as antigen-presentation sites in nonlymphoid peripheral organs. By analogy, the concept of skin-associated lymphoid tissue (SALT) was proposed in the early 1980s, on the basis of findings that cells in the skin are able to capture, process and present antigens[26,27]. However, the role of cellular skin components as antigen-presentation sites has remained uncertain. Here we have identified an inducible structure formed by dermal macrophages, dDCs and effector T cells, which seemed to accumulate sequentially. Because formation of this structure was essential for efficient activation of effector T cells, these inducible leukocyte clusters may function as SALTs. Unlike leukocyte clusters in MALT, these leukocyte clusters were not found in the steady state but were induced during the development of an adaptive immune response. Therefore, these clusters might be better called 'inducible SALTs', similar to inducible BALTs in the lung[28]. In contrast to the cells present in inducible BALT, we did not identify naive T cells or B cells in SALT (data not shown), which suggested that the leukocyte clusters in the skin may be specialized for the activation of effector T cells but not for the activation of naive T cells. Our findings suggest that approaches for the selective inhibition of this structure may have novel therapeutic benefit in inflammatory disorders of the skin.

METHODS

Methods and any associated references are available in the online version of the paper.

Accession codes. GEO: microarray data, GSE53680.

Note: Any Supplementary Information and Source Data files are available in the online version of the paper.

ACKNOWLEDGMENTS

We thank H. Yagita (Juntendo University) for the KBA neutralizing antibody to LFA-1; P. Bergstresser and J. Cyster for critical reading of our manuscript. Supported by grants-in-aid for Scientific Research from the Ministry of Education, Culture, Sports, Science and Technology of Japan.

AUTHOR CONTRIBUTIONS

Y.N., G.E. and K.K. designed this study and wrote the manuscript; Y.N., G.E., S. Nakamizo, S.O., S.H., N.K., A.O., A.K., T. Honda and S. Nakajima performed the experiments and analyzed data; S.T. and Y.S. did experiments related to microarray analysis; K.J.I., H.T., H.Y., Y.I., M.K. and L.g.N. developed experimental reagents and gene-targeted mice; J.F. and E.G.-Y. did experiments related to immunohistochemistry of human samples; T.O., T. Hashimoto, Y.M. and K.K. directed the project and edited the manuscript; and all authors reviewed and discussed the manuscript.

COMPETING FINANCIAL INTERESTS

The authors declare no competing financial interests.

1. von Andrian, U.H. & Mempel, T.R. Homing and cellular traffic in lymph nodes. *Nat. Rev. Immunol.* **3**, 867–878 (2003).
2. Clark, R.A. *et al.* The vast majority of CLA$^+$ T cells are resident in normal skin. *J. Immunol.* **176**, 4431–4439 (2006).
3. Wang, L. *et al.* Langerin expressing cells promote skin immune responses under defined conditions. *J. Immunol.* **180**, 4722–4727 (2008).
4. Tuckermann, J.P. *et al.* Macrophages and neutrophils are the targets for immune suppression by glucocorticoids in contact allergy. *J. Clin. Invest.* **117**, 1381–1390 (2007).
5. Sims, J.E. & Smith, D.E. The IL-1 family: regulators of immunity. *Nat. Rev. Immunol.* **10**, 89–102 (2010).
6. Murphy, J.E., Robert, C. & Kupper, T.S. Interleukin-1 and cutaneous inflammation: a crucial link between innate and acquired immunity. *J. Invest. Dermatol.* **114**, 602–608 (2000).
7. Nakae, S. *et al.* IL-1-induced tumor necrosis factor-α elicits inflammatory cell infiltration in the skin by inducing IFN-γ-inducible protein 10 in the elicitation phase of the contact hypersensitivity response. *Int. Immunol.* **15**, 251–260 (2003).
8. Thyssen, J.P., Linneberg, A., Menne, T., Nielsen, N.H. & Johansen, J.D. Contact allergy to allergens of the TRUE-test (panels 1 and 2) has decreased modestly in the general population. *Br. J. Dermatol.* **161**, 1124–1129 (2009).
9. Ng, L.G. *et al.* Migratory dermal dendritic cells act as rapid sensors of protozoan parasites. *Plos Pathog* **4**, e1000222 (2008).
10. Springer, T.A. & Dustin, M.L. Integrin inside-out signaling and the immunological synapse. *Curr. Opin. Cell Biol.* **24**, 107–115 (2012).
11. Egawa, G. *et al. In vivo* imaging of T-cell motility in the elicitation phase of contact hypersensitivity using two-photon microscopy. *J. Invest. Dermatol.* **131**, 977–979 (2011).
12. Miyawaki, S. *et al.* A new mutation, aly, that induces a generalized lack of lymph nodes accompanied by immunodeficiency in mice. *Eur. J. Immunol.* **24**, 429–434 (1994).
13. Sawaguchi, M. *et al.* Role of mast cells and basophils in IgE responses and in allergic airway hyperresponsiveness. *J. Immunol.* **188**, 1809–1818 (2012).
14. Otsuka, A. *et al.* Requirement of interaction between mast cells and skin dendritic cells to establish contact hypersensitivity. *PLoS ONE* **6**, e25538 (2011).
15. Enk, A.H. & Katz, S.I. Early molecular events in the induction phase of contact sensitivity. *Proc. Natl. Acad. Sci. USA* **89**, 1398–1402 (1992).
16. Weisser, S.B., McLarren, K.W., Kuroda, E. & Sly, L.M. Generation and characterization of murine alternatively activated macrophages. *Methods Mol. Biol.* **946**, 225–239 (2013).
17. Liao, L. *et al.* CXCR2 blockade reduces radical formation in hyperoxia-exposed newborn rat lung. *Pediatr. Res.* **60**, 299–303 (2006).
18. Honda, T., Egawa, G., Grabbe, S. & Kabashima, K. Update of immune events in the murine contact hypersensitivity model: toward the understanding of allergic contact dermatitis. *J. Invest. Dermatol.* **133**, 303–315 (2013).
19. Kaplan, D.H., Igyarto, B.Z. & Gaspari, A.A. Early immune events in the induction of allergic contact dermatitis. *Nat. Rev. Immunol.* **12**, 114–124 (2012).
20. Lee, R.T. *et al.* Mechanical deformation promotes secretion of IL-1 alpha and IL-1 receptor antagonist. *J. Immunol.* **159**, 5084–5088 (1997).
21. Sackstein, R., Falanga, V., Streilein, J.W. & Chin, Y.H. Lymphocyte adhesion to psoriatic dermal endothelium is mediated by a tissue-specific receptor/ligand interaction. *J. Invest. Dermatol.* **91**, 423–428 (1988).
22. Kish, D.D., Gorbachev, A.V. & Fairchild, R.L. IL-1 receptor signaling is required at multiple stages of sensitization and elicitation of the contact hypersensitivity response. *J. Immunol.* **188**, 1761–1771 (2012).
23. Kondo, S. *et al.* Interleukin-1 receptor antagonist suppresses contact hypersensitivity. *J. Invest. Dermatol.* **105**, 334–338 (1995).
24. Cattani, F. *et al.* The role of CXCR2 activity in the contact hypersensitivity response in mice. *Eur. Cytokine Netw.* **17**, 42–48 (2006).
25. Brandtzaeg, P., Kiyono, H., Pabst, R. & Russell, M.W. Terminology: nomenclature of mucosa-associated lymphoid tissue. *Mucosal Immunol.* **1**, 31–37 (2008).
26. Streilein, J.W. Skin-associated lymphoid tissues (SALT): origins and functions. *J. Invest. Dermatol.* **80** (suppl.), 12s–16s (1983).
27. Egawa, G. & Kabashima, K. Skin as a peripheral lymphoid organ: revisiting the concept of skin-associated lymphoid tissues. *J. Invest. Dermatol.* **131**, 2178–2185 (2011).
28. Moyron-Quiroz, J.E. *et al.* Role of inducible bronchus associated lymphoid tissue (iBALT) in respiratory immunity. *Nat. Med.* **10**, 927–934 (2004).

ONLINE METHODS

Mice. 8- to 12-week-old female C57BL/6 mice were used in this study. C57BL/6N mice were from SLC. Langerin-eGFP-DTR mice[29], CD11c-DTR mice[30], CD11c-YFP mice (that express CD11c tagged with YFP)[31], LysM-DTR mice[32], RAG-2-deficient mice[33], Mas-TRECK mice[13,14], Bas-TRECK mice[13,14], ALY/NscJcl- aly/aly mice[12], IL-1α/β-deficient mice[34], IL-1R1-deficient mice[35], NLRP3-deficient mice[36] and caspase-1/11-deficient mice[37] have been described. All experimental procedures were approved by the Institutional Animal Care and Use Committee of Kyoto University Graduate School of Medicine.

Human subjects. Biopsy samples of human skin were obtained from a nickel-reactive patch after 48 h after placement of nickel patch tests in patients with previously proven allergic contact dermatitis. A biopsy of petrolatum-occluded skin was also obtained as a control. Informed consent was obtained under protocols approved by the Institutional Review Board at the Icahn School of Medicine at Mount Sinai School Medical Center, and the Rockefeller University in New York.

Induction of CHS responses. Mice were sensitized on shaved abdominal skin with 25 μl 0.5% (wt/vol) DNFB (1-fluoro-2,4-dinitrofluorobenzene ; Nacalai Tesque) dissolved in acetone and olive oil (at a ratio of 4:1). Five days later, the ears were challenged with 20 μl 0.3% DNFB. For adoptive transfer, T cells were magnetically sorted, with an autoMACS (Miltenyi Biotec), from the draining LNs of sensitized mice and then were transferred intravenously (1×10^7 cells) into naive mice.

Depletion of cutaneous DC subsets, macrophages and neutrophils. For depletion of all cutaneous DC subsets (including LCs), 6-week-old Langerin-DTR mice were irradiated (two doses of 550 rads given 3 h apart) and were given transfer of 1×10^7 BM cells from CD11c-DTR mice. Eight weeks later, 2 μg DT (Sigma-Aldrich) was injected intraperitoneally. For selective depletion of LCs, irradiated Langerin-DTR mice were given transfer of BM cells from C57BL/6 mice, and 1 μg DT was injected. For selective depletion of dDCs, irradiated C57BL/6 mice were given transfer of BM cells from CD11c-DTR mice, and 2 μg DT was injected. For depletion of macrophages, irradiated C57BL/6 mice were given transfer of BM cells from LysM-DTR mice and 800 ng DT was injected. For depletion of neutrophils, anti-Ly6G (1A8; BioXCell) was administered to mice intravenously at a dose of 0.5 mg per mouse 24 h before experiments.

Time-lapse imaging of cutaneous DCs, macrophages and T cells. Cutaneous DCs were observed in CD11c-YFP mice. For labeling of cutaneous macrophages *in vivo*, 5 mg TRITC-dextran (Sigma-Aldrich) was injected intravenously and mice were allowed to 'rest' for 24 h. At that time, cutaneous macrophages became fluorescent because they had incorporated extravasated dextran. For labeling of skin-infiltrating T cells, T cells from DNFB-sensitized mice were labeled with CellTracker Orange (CMTMR (5-(and-6)-(((4-chloromethyl)benzoyl) amino)tetramethylrhodamine); Invitrogen) and were adoptively transferred into recipient mice. Keratinocytes and sebaceous glands were visualized by subcutaneous injection of isolectin B4 (Invitrogen) and BODIPY (Molecular Probes), respectively. Mice were positioned on a heating plate on the stage of a two-photon IX-81 microscope (Olympus) and their ear lobes were fixed beneath a cover slip with a single drop of immersion oil. Stacks of ten images, spaced 3 μm apart, were acquired at intervals of 1–7 min for up to 24 h. For calculation of T cell and DC velocities, movies were processed and analyzed with Imaris 7.2.1 software (Bitplane).

Histology and immunohistochemistry. For histological examination, tissues were fixed with 10% formalin in phosphate-buffered saline, then were embedded in paraffin. Sections with a thickness of 5 μm were prepared and then were stained with hematoxylin and eosin. For whole-mount staining, the ears were split into dorsal and ventral halves and were incubated for 30 min at 37 °C with 0.5 M ammonium thiocyanate. Then the dermal sheets were separated and fixed in acetone for 10 min at −20 °C. After treatment with Image-iT FX Signal Enhancer (Invitrogen), the sheets were incubated with antibody to mouse MHC class II (M5/114.15.2; eBioscience) followed by incubation with antibody to rat IgG conjugated to Alexa Fluor 488 (A-11006; Invitrogen) or Alexa Fluor 594 (A-11007; Invitrogen). The slides were mounted with a ProLong Antifade kit with the DNA-binding dye DAPI (4′6-diamidino-2-phenylindole; Molecular Probes) and were observed with a fluorescent microscope (BZ-900; KEYENCE). The number and size of DC clusters were evaluated in ten fields of 1 mm^2 per ear and were assigned scores according to the criteria in **Supplementary Figure 5a**.

Cell isolation and flow cytometry. For the isolation of skin lymphocytes, the split ears were incubated for 1 h at 37 °C in digestion buffer (RPMI medium supplemented with 2% FCS, 0.33 mg/ml of Liberase TL (Roche) and 0.05% DNase I (Sigma-Aldrich)). After that incubation, the tissues were disrupted by passage through a 70-μm cell strainer and stained with the appropriate antibodies (identified below). For analysis of intracellular cytokine production, cell suspensions were obtained in the presence of 10 μg/ml of brefeldin A (Sigma-Aldrich) and were fixed with Cytofix Buffer and permeabilized with Perm/Wash Buffer according to the manufacturer's protocol (BD Biosciences). Cells were stained with the following: antibody to mouse CD4 (GK1.5), anti-CD8 (53-6.7), anti-CD11b (M1/70), anti-CD11c (N418), anti-B220 (RA3-6B2), antibody to MHC class II (M5/114.15.2), anti-F4/80 (BM8), anti-IFN-γ (XMG1.2), anti-Gr1 (RB6-8c5) and 7-amino-actinomycin D (all from eBioscience); anti-mouse CD45 (30-F11) and anti-TCR-β (H57-597; both from BioLegend); and anti-CD16-CD32 (2.4G2; BD Biosciences). Flow cytometry was done with an LSR Fortessa (BD Biosciences) and data were analyzed with FlowJo software (TreeStarA).

Chemotaxis assays. Chemotaxis was assessed as described with some modifications[38]. The dermis of the ear skin was minced and then was digested for 30 min at 37 °C with 2 mg/ml collagenase type II (Worthington Biochemical) containing 1 mg/ml hyaluronidase (Sigma-Aldrich) and 100 μg/ml DNase I (Sigma-Aldrich). DDCs and macrophages were isolated with an autoMACS. Alternatively, BM-derived DCs and macrophages were prepared. 1×10^6 DCs were added to a Transwell insert with a pore size of 5 μm (Corning), and 5×10^5 macrophages were added to the lower wells, and the cells were incubated for 12 h at 37 °C. A known number of fluorescent reference beads (FlowCount fluorospheres; Beckman Coulter) were added to each sample to allow accurate quantification of cells that had migrated to the lower wells by flow cytometry.

Cell proliferation assay. Mice were sensitized with 25 μl 0.5% DNFB or 7% trinitrochlorobenzene (Chemical Industry). Five days later, T cells were magnetically separated from the draining LNs of each group of mice and were labeled with CellTrace Violet according to the manufacturer's protocol (Invitrogen). 1×10^6 T cells were adoptively transferred into naive mice, and the ears of the recipient mice were challenged with 20 μl of 0.5% DNFB. 24 h later, ears were collected and analyzed by flow cytometry.

***In vitro* differentiation of DCs and M1 and M2 macrophages from BM cells.** BM cells from the tibias and fibulas were plated at a density of 5×10^6 cells per 10-cm dish on day 0. For DC differentiation, cells were cultured at 37 °C in 5% CO_2 in cRPMI medium (RPMI medium supplemented with 1% L-glutamine, 1% HEPES, 0.1% 2-mercaptoethanol and 10% FBS) containing 10 ng/ml granulocyte-macrophage colony-stimulating factor (Peprotech). For macrophage differentiation, BM cells were cultured in cRPMI medium containing 10 ng/ml macrophage colony-stimulating factor (Peprotech). The medium was replaced on days 3 and 6 and cells were harvested on day 9. For the induction of M1 macrophages or M2 macrophages, cells were stimulated for 48 h with IFN-γ (10 ng/ml; R&D Systems) or with IL-4 (20 ng/ml; R&D Systems), respectively.

***In vitro* IL-1α-stimulation assay of dermal macrophages.** Dermal macrophages were separated from mice deficient in IL-1α and IL-1β[34] to avoid preactivation during cell preparations. Split ears were treated for 30 min at 37 °C with 0.25% trypsin and EDTA for removal of the epidermis, then were minced and then incubated with collagenase as described above. $CD11b^+$ cells were separated by magnetic-activated cell sorting, and 2×10^5 cells per well in 96-well plates were incubated for 24 h with or without 10 ng/ml IL-1α (R&D Systems).

doi:10.1038/ni.2992

Blocking assay. For the LFA-1-blocking assay, mice were given intravenous injection of 100 μg KBA (neutralizing antibody to LFA-1; a gift from H. Yagita) 12–14 h after challenge with 20 μl 0.5% DNFB. For blockade of IL-1R, mice were given subcutaneous injection of 10 μg recombinant mouse IL-1ra (PROSPEC) 5 h before challenge. For blockade of CXCR2, mice were given intraperitoneal treatment with 50 μg CXCR2 inhibitor[17] (SB265610; Tocris Bioscience) 6 h before and at the time of painting of the skin with hapten.

Quantitative PCR analysis. Total RNA was isolated with an RNeasy Mini kit (Qiagen, Hilden, Germany). cDNA was synthesized with a PrimeScript RT reagent kit and random hexamers according to the manufacturer's protocol (TaKaRa). A LightCycler 480 and LightCycler SYBR Green I Master mix were used according to the manufacturer's protocol (Roche) for quantitative PCR (primer sequences, **Supplementary Table 2**). The expression of each gene was normalized to that of the control gene *Gapdh*.

Microarray analysis. Total RNA was isolated with an RNeasy Mini Kit according to the manufacturer's protocol (Qiagen). An amplified sense-strand DNA product was synthesized with the Ambion WT Expression Kit (Life Technologies), was fragmented and labeled by the WT Terminal Labeling and Controls Kit (Affymetrix) and was hybridized to a Mouse Gene 1.0 ST Array (Affymetrix). We used the robust multiarray average algorithm for log transformation ($\log_2$) and normalization of the GeneChip data.

General experimental design and statistical analysis. For animal experiments, a sample size of three to five mice per group was used on the basis of past experience in generating statistical significance. Mice were randomly assigned to study groups and no specific randomization or blinding protocol was used. Sample or mouse identity was not masked for any of these studies. Prism software (GraphPad) was used for statistical analyses. Normal distribution was assumed a priori for all samples. Unless indicated otherwise, an unpaired parametric *t*-test was used for comparison of data sets. In cases in which the data-point distribution was not Gaussian, a nonparametric *t*-test was also applied. *P* values of less than 0.05 were considered significant.

29. Kissenpfennig, A. *et al.* Dynamics and function of Langerhans cells *in vivo*: dermal dendritic cells colonize lymph node areas distinct from slower migrating Langerhans cells. *Immunity* **22**, 643–654 (2005).
30. Jung, S. *et al. In vivo* depletion of CD11c$^+$ dendritic cells abrogates priming of CD8$^+$ T cells by exogenous cell-associated antigens. *Immunity* **17**, 211–220 (2002).
31. Lindquist, R.L. *et al.* Visualizing dendritic cell networks *in vivo*. *Nat. Immunol.* **5**, 1243–1250 (2004).
32. Miyake, Y. *et al.* Protective role of macrophages in noninflammatory lung injury caused by selective ablation of alveolar epithelial type II Cells. *J. Immunol.* **178**, 5001–5009 (2007).
33. Hao, Z. & Rajewsky, K. Homeostasis of peripheral B cells in the absence of B cell influx from the bone marrow. *J. Exp. Med.* **194**, 1151–1164 (2001).
34. Horai, R. *et al.* Production of mice deficient in genes for interleukin (IL)-1α, IL-1β, IL-1α/β, and IL-1 receptor antagonist shows that IL-1β is crucial in turpentine-induced fever development and glucocorticoid secretion. *J. Exp. Med.* **187**, 1463–1475 (1998).
35. Coban, C. *et al.* Immunogenicity of whole-parasite vaccines against *Plasmodium falciparum* involves malarial hemozoin and host TLR9. *Cell Host Microbe* **7**, 50–61 (2010).
36. Martinon, F., Petrilli, V., Mayor, A., Tardivel, A. & Tschopp, J. Gout-associated uric acid crystals activate the NALP3 inflammasome. *Nature* **440**, 237–241 (2006).
37. Koedel, U. *et al.* Role of caspase-1 in experimental pneumococcal meningitis: evidence from pharmacologic caspase inhibition and caspase-1-deficient mice. *Ann. Neurol.* **51**, 319–329 (2002).
38. Tomura, M. *et al.* Activated regulatory T cells are the major T cell type emigrating from the skin during a cutaneous immune response in mice. *J. Clin. Invest.* **120**, 883–893 (2010).

doi:10.1038/ni.2992

Vaccine 32 (2014) 5607–5613

Contents lists available at ScienceDirect

Vaccine

journal homepage: www.elsevier.com/locate/vaccine

Protective properties of a fusion pneumococcal surface protein A (PspA) vaccine against pneumococcal challenge by five different PspA clades in mice

Zhenyu Piao[a,b], Yukihiro Akeda[a], Dan Takeuchi[a], Ken J. Ishii[c,d], Kimiko Ubukata[e], David E. Briles[g], Kazunori Tomono[b], Kazunori Oishi[f,*]

[a] Laboratory for Clinical Research on Infectious Disease, International Research Center for Infectious Diseases, Research Institute for Microbial Diseases, Osaka University, Japan
[b] Division of Infection Control and Prevention, Osaka University Graduate School of Medicine, Japan
[c] National Institute of Biomedical Innovation, Japan
[d] Laboratory of Vaccine Science, WPI Immunology Frontier Research Center, Osaka University, Japan
[e] Department of Infectious Diseases, Keio University School of Medicine, Japan
[f] Infectious Disease Surveillance Center, National Institute of Infectious Diseases, Japan
[g] Department of Microbiology, University of Alabama at Birmingham, USA

ARTICLE INFO

Article history:
Received 12 May 2014
Received in revised form 21 July 2014
Accepted 31 July 2014
Available online 12 August 2014

Keywords:
Streptococcus pneumoniae
PspA fusion protein
PspA vaccine
Cross-protection
Binding of PspA-specific IgG

ABSTRACT

An increase in the appearance of nonvaccine serotypes in both children and adults with invasive pneumococcal disease (IPD) after introduction of pneumococcal conjugate vaccine represents a limitation of this vaccine. In this study, we generated three recombinant pneumococcal surface protein A (PspA) proteins comprising PspA families 1 and 2, and we examined the reactivity of antisera raised in mice immunized with a PspA fusion protein in combination with CpG oligonucleotides plus aluminum hydroxide gel. The protective effects of immunization with PspA fusion proteins against pneumococcal challenge by strains with five different PspA clades were also examined in mice. Flow cytometry demonstrated that PspA3+2-induced antiserum showed the greatest binding of PspA-specific IgG to all five challenge strains with different clades. PspA2+4- or PspA2+5-induced antiserum showed the lowest binding of PspA-specific IgG to clade 3. Immunization with PspA3+2 afforded significant protection against pneumococcal challenge by five strains with different clades in mice, but immunization with PspA2+4 or PspA2+5 failed to protect mice from pneumococcal challenge by strains with clades 1 and 3. The binding of PspA-specific IgG in antisera raised by three PspA fusion proteins was examined in 68 clinical isolates from adult patients with IPD. Immunization of mice with PspA3+2-induced antiserum with a high binding capacity for clinical isolates expressing clades 1–4, but not clade 5. Our results suggest that the PspA3+2 vaccine has an advantage over the PspA2+4 or PspA2+5 vaccine in terms of a broad range of cross-reactivity with clinical isolates and cross-protection against pneumococcal challenge in mice.

1. Introduction

Streptococcus pneumoniae is a major cause of morbidity and mortality caused by pneumonia, bacteremia, and meningitis worldwide [1]. After introduction of the seven-valent pneumococcal conjugate vaccine (PCV7) in children, significant declines in the incidence of invasive pneumococcal disease (IPD) caused by vaccine serotypes were reported in children and adults [2,3]. However, an increase in the incidence of IPD caused by non-PCV7 serotypes has been also observed in children and adults [3–5]. In addition, after introduction of a 13-valent pneumococcal conjugate vaccine (PCV13) in children, serotypes not included in PCV13 have been isolated with increasing frequency in pediatric and adult patients with IPD [6,7]. Because there are >90 different pneumococcal capsular serotypes, continuous supplementation of pneumococcal conjugate vaccines with new serotypes for serotype replacement may not be a practical strategy.

Previous studies have demonstrated that several pneumococcal proteins are potential vaccine candidates [8–11]. One candidate protein antigen is pneumococcal surface protein A (PspA), which is

* Corresponding author. Tel.: +81 3 5285 1111; fax: +81 3 5285 1129.
E-mail address: oishik@nih.go.jp (K. Oishi).

http://dx.doi.org/10.1016/j.vaccine.2014.07.108
0264-410X/